Downloaded from https://www.lyellcollection.org by UK Research and Innovation (UKRI/BGS/BAS) on Mar 09, 2026

Accepted Manuscript

Geoenergy

Evaluation of the Röt Halite Member as a top seal for carbon dioxide storage in the Southern North Sea

H. A. Morris, J. D. O. Williams, L. E. Abel, E. Hough, L. P. Field & R. Parsons

DOI: https://doi.org/10.1144/geoenergy2025-029

To access the most recent version of this article, please click the DOI URL in the line above. When citing this article please include the above DOI.

This article is part of the Characterization and monitoring of containment in subsurface CO_2 storage collection available at: https://www.lyellcollection.org/topic/collections/containment

Received 16 June 2025
Revised 4 December 2025
Accepted 23 January 2026

© 2026 UKRI. The British Geological Survey.. This is an Open Access article distributed under the terms of the Creative Commons Attribution License (https://creativecommons.org/licenses/by/4.0/). Published by The Geological Society of London for GSL and EAGE. Publishing disclaimer: https://www.lyellcollection.org/publishing-hub/publishing-ethics

Supplementary material at https://doi.org/10.6084/m9.figshare.c.8272578

Manuscript version: Accepted Manuscript
This is a PDF of an unedited manuscript that has been accepted for publication. The manuscript will undergo copyediting, typesetting and correction before it is published in its final form. Please note that during the production process errors may be discovered which could affect the content, and all legal disclaimers that apply to the journal pertain.

Although reasonable efforts have been made to obtain all necessary permissions from third parties to include their copyrighted content within this article, their full citation and copyright line may not be present in this Accepted Manuscript version. Before using any content from this article, please refer to the Version of Record once published for full citation and copyright details, as permissions may be required.

Downloaded from https://www.lyellcollection.org by UK Research and Innovation (UKRI/BGS/BAS) on Mar 09, 2026

Evaluation of the Röt Halite Member as a top seal for carbon dioxide storage in the Southern North Sea

Top seal characteristics of the Röt Halite Member

H. A. Morris[1], J. D. O. Williams[1]*, L. E. Abel[1], E. Hough[1], L. P. Field[1], R. Parsons[1]

[1]British Geological Survey, Nicker Hill, Keyworth, Nottingham, NG12 5GG

*Correspondence: jdow@bgs.ac.uk

H.A.M. https://orcid.org/0009-0003-3912-8423

J.D.O.W. https://orcid.org/0000-0003-0177-9848

L.E.A. https://orcid.org/0009-0006-4109-0163

E.H. https://orcid.org/0000-0002-2555-3969

L.P.F. https://orcid.org/0000-0002-8747-9901

Abstract

The Röt Halite Member (RHM) is a top seal for planned carbon dioxide (CO_2) storage operations in the Bunter Sandstone Formation of the UK Southern North Sea (UKSNS). While previous studies have considered that the RHM, where present, is likely to provide an effective top seal for CO_2 storage, few have investigated the RHM in detail to determine its top seal characteristics on a regional scale. Downhole petrophysical logs reveal a distinct, regionally extensive evaporite cyclicity with up to five halite-mudstone-dolomite/anhydrite sequences. These have been mapped across the UKSNS using an extensive catalogue of 600 wells, providing insight into the extent, distribution and thickness of the individual evaporite cycles. The mapping reveals the depositional history of the RHM in the UKSNS, with initial flooding, subsequent expansion and eventual contraction of the evaporite basin. The depositional model is supported by petrographic interpretation from an RHM thin section sample. Additional datasets, including seismic reflection data are also reviewed to complement a discussion on the potential impacts on long-term containment and to identify remaining uncertainties. This regional understanding allows more detailed site-specific containment risk studies, in support of the CO_2 licencing and permitting process, to be placed within an appropriate regional context.

ACCEPTED MANUSCRIPT

Downloaded from https://www.lyellcollection.org by UK Research and Innovation (UKRI/BGS/BAS) on Mar 09, 2026

Introduction

The long-term containment of CO_2 in the subsurface is an essential requirement of Carbon Capture and Storage (CCS) projects (EC, 2009; HMSO, 2010; OPC, 2011; IEAGHG, 2011; ISO, 2017). The presence of an effective top seal formation is therefore one of the principal considerations in any containment risk assessment for proposed storage sites. Common CO_2 storage concepts include storage in saline aquifer formations and produced hydrocarbon fields. Whilst CO_2 and hydrocarbon fluids exhibit differences in fluid densities, interfacial tension and wettability (Davis et al., 2024; Iglauer et al., 2015; Span and Wagner, 1996), the effectiveness of top seals in hydrocarbon traps is proven to an extent by the trapping of buoyant hydrocarbon columns over geological time. Additionally, knowledge of top seal characteristics is acquired during the hydrocarbon exploration and appraisal process. Further information, such as changes in pressure and fluid composition is commonly acquired as the pressure system evolves during production, enabling top seal behaviour to be observed. In contrast, relatively little observational evidence for top seal effectiveness is available for saline aquifer storage systems. A rigorous approach to data collection and the adoption of model-led approaches to interpretation is therefore required during CO_2 storage appraisal in saline aquifer formations (Shoulders and Hodgkinson, 2024).

There is significant potential for CO_2 storage in the UK Southern North Sea (UKSNS), where the principal storage plays include subsalt depleted gas fields (Permian) and Triassic saline aquifer reservoirs within suprasalt structures (Underhill et al., 2023). The Early Triassic Bunter Sandstone Formation (BSF) has emerged as an important saline aquifer storage unit in the UK Southern North Sea (UKSNS) where it provides a principal target reservoir in several carbon storage licences (Figure 1). The presence of large structural closures coupled with a thick (up to ~350 m) and high net-to-gross reservoir has led to consideration of the BSF as a major saline aquifer storage target in the UKSNS. The BSF offers potential opportunities for several storage concepts, including closed saline aquifer structures (or brine-filled traps), migration-assisted trapping, and storage in produced gas fields (Holloway et al., 2006; Hollinsworth et al., 2022; de Jonge-Andersen et al., 2022; Patruno et al., 2024). The geological characteristics of the BSF as a reservoir unit in relation to CO_2 storage are described in detail elsewhere (Abel et al., 2025; Bentham et al., 2013, 2017; de Jonge-Anderson et al., 2022; Gibson-Poole et al., 2024; Hollinsworth et al., 2022; 2024; Hossain et al., 2024; Rushton et al., 2025; Williams et al., 2013a; 2013b; 2014) and are not the focus of this study.

[Figure 1]

Several dynamic simulation studies have investigated the impacts of CO_2 injection in parts of the BSF (Agada et al., 2017; Heinemann et al. 2012; Noy et al. 2012; Hannis et al., 2013; Williams et al.,

ACCEPTED MANUSCRIPT

Downloaded from https://www.lyellcollection.org by UK Research and Innovation (UKRI/BGS/BAS) on Mar 09, 2026

2013b). These studies indicate that while CO_2 stored in structural closures is expected to be trapped locally due to buoyancy effects, the laterally extensive nature of the BSF means that pressure responses, resulting from the displacement of brine, may be felt far more widely beyond the limits of CO_2 storage sites. Consequently, it is important to understand the continuity and properties (e.g. lithological, capillary and mechanical characteristics) of the top seal formations beyond the expected extent of CO_2 plumes. In the case of the BSF, major post-depositional structural lineaments divide the BSF into distinct, yet extensive, hydraulic units (Abel et al., 2025). The scale of these hydraulic units, of the order of more than 10,000 km^2, highlights the importance of top seal characterisation at the regional scale.

The Haisborough Group forms the primary top seal for the BSF over most of the UKSNS, except where it is removed by erosion beneath the Base Cretaceous Unconformity on the margins of the Cleaver Bank High (Figure 1 and Figure 2). The Haisborough Group comprises a thick playa mudflat and distal floodplain sequence with intercalated units deposited in hypersaline shallow quasi-marine environments (Cameron et al., 1992). Whilst the Haisborough Group predominantly comprises red estuarine and loessic mudstone, substantial intercalations of marine evaporite and coastal sabkha deposits are also present. Three halite-bearing members are regionally developed across much of the UKSNS, each representing a temporary marine influx across the basin, emanating from the east (Cameron et al., 1992). The earliest of these is the Röt Halite Member (RHM), which overlies the BSF near the base of the Dowsing Formation (Figure 2). A thin claystone, laterally equivalent to the Solling Formation of the Netherlands and colloquially termed the Röt Clay (Furnival et al., 2014; Hollinsworth et al., 2022; Gibson-Poole et al., 2024), separates the RHM from the BSF below. The RHM and underlying Röt Clay in the UKSNS are Anisian in age (Salisbury et al., 2023) and are separated from the underlying BSF by the Hardegsen Unconformity (Figure 2). Where these halites are present they are expected to enhance the sealing characteristics of the Haisborough Group. This is because of the unique properties of halite such as its extremely low permeability and its mechanical behaviour which enables self-sealing of potential flow pathways (Warren, 2017).

[Figure 2]

The RHM is primarily comprised of bedded halite in up to five cycles of deposition (Southworth, 1987) and is present across a significant portion of the UKSNS where it is typically around 30–80 m thick. Because of this, and the widely recognised effectiveness of halite as a mechanical and capillary top seal (Warren, 2016; Davis et al., 2024), it is commonly assumed that where present, the RHM is likely to form an effective seal for CO_2 storage (Heinemann et al., 2012; Williams et al., 2014; Hollinsworth et al., 2022). Beyond this, few studies have investigated the RHM in detail to determine

ACCEPTED MANUSCRIPT

Downloaded from https://www.lyellcollection.org by UK Research and Innovation (UKRI/BGS/BAS) on Mar 09, 2026

the lateral continuity of the bedded halite units and their likely characteristics as a top seal for CO_2 storage on a regional scale. This study first presents a detailed evaluation of the extent, distribution and thickness of individual evaporite cycles within the RHM using petrophysical logs, primarily acquired during legacy oil and gas exploration and development activities. Areas in which the continuity of the RHM is disturbed by post-depositional faulting or invasion by older, mobile Zechstein evaporites are also identified. These observations are then discussed in the context of seal effectiveness for future CO_2 storage operations in the UKSNS. A secondary objective of the study is to provide a review of supplementary information that relates to the potential of the RHM as a top seal. Given that few studies have evaluated the characteristics of the RHM in the UKSNS in detail, this review provides a summary of the understanding to date based both on new analysis presented in this study combined with information from literature sources. Areas where further knowledge is required are also highlighted to inform future appraisal activities. The review includes a petrographic analysis of a sample from the 42/25d-3 CO_2 storage appraisal well, which was drilled to appraise the Endurance storage site in 2013 (Furnival et al, 2014; Gluyas and Bagudu, 2020; Gibson-Poole et al., 2024). This is provided to complement understanding of the depositional environment. Observations from a previous seismic interpretation study (Abel et al., 2025) are also described to provide further understanding of the RHM's influence on post-depositional deformation of the BSF and its top seal. Finally, geomechanical considerations are discussed in view of information and understanding available from the literature. Overall, this study provides a regional understanding of the RHM in which further detailed site-specific containment risk studies can be constrained, while also highlighting some knowledge gaps that could be addressed during CO_2 storage appraisal activities.

Geological setting

Regional context

The UKSNS comprises the western part of the Southern Permian Basin (SPB), a broadly west to east trending area of subsidence which extends from the east of the UK as far as Poland and the Baltic States (Cameron et al., 1992; Doornenbal and Stevenson, 2010). While the Pennine High controlled the western extent of the SPB, the UKSNS region was also bound to the north by the Mid North Sea High, and to the south by the London Brabant Massif. Detailed accounts of the structure, stratigraphy and petroleum system of the UKSNS are given by Cameron et al. (1992), Underhill (2003), Doornenbal and Stevenson (2010) and Brackenridge et al. (2020). Only the features relevant to Early to Middle Triassic deposition and subsequent deformation are detailed here.

A generalised stratigraphy for the basin is shown in Figure 2. Following the last of the Permian marine incursions that led to the deposition of the Zechstein Supergroup, the evaporite basin rapidly

ACCEPTED MANUSCRIPT

Downloaded from https://www.lyellcollection.org by UK Research and Innovation (UKRI/BGS/BAS) on Mar 09, 2026

contracted and continental conditions were established across the UKSNS region. Arid to semi-arid conditions subsequently prevailed during the Early to Mid-Triassic. During these times, the Tethys Ocean occupied an equatorial position, flanked by large continental masses to the north and south (Parrish, 1993). Consequently, strongly seasonal monsoonal conditions prevailed with significant precipitation over the remnant Variscan mountains in south-central Europe and Iberia. This resulted in development of the Triassic River System which drained northwards towards northern Europe and the endorheic UKSNS drainage basin (Parrish, 1993). The BSF forms the upper part of the Bacton Group and represents the terminus of the Triassic River System in the UKSNS (Newell, 2018). While subsequent halokinesis has somewhat obscured the existence of pre-existing fault topography, sediment thickness changes indicate that a prominent depocentre was active in the Sole Pit Trough from Early Triassic times (Cameron et al., 1992; Hollinsworth et al., 2024). Stratigraphic thickness changes observed in Middle to Late Triassic strata suggest that syn-sedimentary faults were particularly active during deposition (Allen et al. 1994; Griffiths et al. 1995). It has been suggested that observed thickness changes in the lowermost Haisborough Group units resulted from dextral wrenching along the Dowsing Fault Zone and other northwest-southeast trending fault zones, potentially associated with the initial opening of the Central Graben (Southworth, 1987).

Deposition of the RHM represents the first major connection of the UKSNS to the Tethys Ocean, with sea water from the east entering the basin via restricted connections through the Silesian-Moravian and East Carpathian gateways in southern Poland (Ziegler, 1990; Geluk, 2005). A marine connection to the equivalent RHM halite formation in the Netherlands has been shown by Holser and Wilgus (1981). In addition, Kovalevych et al. (2002) showed that RHM brine composition is consistent across Poland, Germany and the Netherlands. Ruffell and Hounslow (2006) note that there is some debate regarding the causative mechanism behind the marine incursions that led to deposition of the RHM. Paleoclimatic changes, eustatic sea-level rise and regional tectonism have all previously been invoked (Ruffell and Hounslow, 2006), with all these processes likely having an influence locally. Southworth (1987) proposed that the overall expansion and subsequent contraction of the Triassic evaporite basin most likely resulted from an overall period of eustatic sea level rise and fall rather than episodic opening of the tectonic gateways near the entrance to Tethys. Intra-RHM evaporite cyclicity would have resulted from smaller-scale and more locally developed fluctuations. Evidence presented in support of eustatic rather than tectonic controls include the asymmetrical distribution of the individual evaporite cycles together with frequent cyclicity exhibited throughout deposition of the Dowsing Formation (Southworth, 1987). Southworth (1987) also notes the strong correlation between the transgression/regression cycles within the basin with the global coastal onlap charts of Haq et al. (1987).

ACCEPTED MANUSCRIPT

Downloaded from https://www.lyellcollection.org by UK Research and Innovation (UKRI/BGS/BAS) on Mar 09, 2026

The RHM was deposited in a series of linked, hypersaline brine pans. Where the RHM is present onshore in eastern England, lateral thickness changes have been attributed to the development of discrete structural highs separating depositional areas, rather than the development of halokinesis (Riddler, 1981). While outcrop is absent, information regarding the depositional environment of the evaporites can be determined from borehole samples such as rock cores and drill cuttings, when available. Riddler (1981) describes the RHM as comprising clear halite which is pink towards its base and contains some impure silty beds. Where present, siltstone/mudstone beds are grey-green in colour and a thin basal anhydritic/dolomitic mudstone bed is present. The RHM is easily differentiated in core and from downhole petrophysical logs by the presence of halite, relative to the red-brown, playa-lake mudstone of the lowermost Dowsing Formation. Southworth (1987) recognised five evaporite cycles within the RHM (A–E), each separated by a thin mudstone overlain by a thin bed of dolomite or anhydrite. Each halite cycle resulted from a rapid marine transgression followed by a gradual marine regression.

Refined stratigraphy

Figure 3 presents a comparison between the stratigraphic interpretation of Southworth (1987), the formalised lithostratigraphy in the UK (Johnson et al., 1994), and the stratigraphic nomenclature in the Netherlands (Geluk and Röhling, 1997). Southworth (1987) proposed a stratigraphic and paleoenvironmental model for the Dowsing Formation, which identified several distinct units not recognised in the formalised UK stratigraphic scheme. In the context of assessing the RHM as a top seal for CO_2 storage, the additional detail afforded by the Southworth (1987) and Geluk and Röhling, (1997) models enables an enhanced discussion of lithological variations and their distribution. The formally recognised RHM of Johnson et al. (1994) corresponds to the Main Röt Halite Member of Southworth (1987). The RHM is overlain by a sabkha facies comprising an interbedded sequence of anhydrites, dolomites and dolomitic mudstone, which overstep the RHM towards the landward margins. Both the Main Röt Halite Member (here referred to as RHM) and Main Röt Evaporite Member identified by Southworth (1987) are included as part of the Main Röt Evaporite Member of the Netherlands. An Upper Röt Halite unit is also recognised, indicating a second major marine incursion and subsequent regression. The Upper Röt Halite is restricted to the central part of the basin where it attains a maximum thickness of about 11 m (Cameron et al., 1992). Similarly to the RHM, it is also overlain and overstepped by marginal evaporitic facies comprising an interbedded sequence of anhydrite, dolomite and dolomitic mudstone. Historical well records are inconsistent in the placement of the top RHM, variably identifying it at the top of the Main Röt Halite, Main Röt Evaporite, Upper Röt Halite or Upper Röt Evaporite units of Southworth (1987).

ACCEPTED MANUSCRIPT

Downloaded from https://www.lyellcollection.org by UK Research and Innovation (UKRI/BGS/BAS) on Mar 09, 2026

[Figure 3]

Review of seal capacity studies

The general lack of a connected pore architecture in halite precludes measurement of typical flow properties such as permeability and capillary pressure using fluids such as helium or mercury. Where estimated in specialist studies using methods such as the argon gas transient step method or steady flow rate and pulse technique using nitrogen gas (Peach and Spiers, 1996; Popp et al., 2001; Schulze et al., 2001), the permeability of undisturbed halite is attributed in the nanodarcy (10^{-6} mD) range but can be several orders of magnitude lower (Warren, 2017). In addition to the very low estimates of permeability and high entry pressures, halite is highly ductile. Its ability to stream, re-anneal and re-establish lattice bonding via pressure-solution creep reduces the susceptibility of halite to fracturing during deformation (Warren, 2017). In addition, given its limited ability to sustain shear stresses, halite has near isotropic *in situ* stress, and therefore very high mechanical seal capacities (Warren, 2016). Brittle fracturing does occur and is generally restricted to situations with very high strain rates, with resulting fractures typically annealing (Davison, 2009). In many basins globally, the excellent sealing capacity of halite is demonstrated by its proven ability to maintain significant pressure differentials across halite barriers. The Permian evaporites of the Zechstein Group form highly effective top seals for natural gas accumulations in underlying reservoirs in the UKSNS. Seal integrity in the Triassic East Irish Sea Basin has also been shown to be excellent where the Triassic reservoirs are overlain by halite-dominated intervals in the Mercia Mudstone Group (Seedhouse and Racey, 1997), which is laterally equivalent to the Haisborough Group. Similarly, Triassic bedded halite units in the Cheshire Basin have been used for the development of engineered salt caverns for natural gas storage (Evans et al., 2009), while the presence of gas accumulations in the BSF indicate effective trapping of hydrocarbons in the UKSNS (Williams et al., 2014).

Whilst no direct capillary pressure measurements are available for the RHM, a small number of measurements are available from formations analogous to the lowermost Haisborough Group units from nearby basins. These studies indicate that hydrocarbon gas columns (methane) of several hundreds of metres can be retained beneath the top seals (Armitage et al., 2013; Seedhouse and Racey, 1997; Spain and Conrad, 1997). Empirical evidence for the seal effectiveness of the Röt Clay and RHM is provided by the small number of natural gas fields in the UKSNS where the BSF provides the reservoir (such as the Esmond, Forbes and Gordon fields). Maximum overpressures induced by the presence of buoyant gas columns, that are retained by the top seal are in the region of 1.1 MPa (Williams et al., 2014). Although this provides an empirically derived lower bounding value, it does not necessarily reflect the true sealing capacity of the RHM for several reasons. Firstly, the RHM is

ACCEPTED MANUSCRIPT

Downloaded from https://www.lyellcollection.org by UK Research and Innovation (UKRI/BGS/BAS) on Mar 09, 2026

underlain by the Röt Clay which has been shown to be capable of supporting pressure differentials up to c. 10 MPa (Bentham et al., 2017), and as such the overpressure is not necessarily exerted at the base of the RHM. Secondly, gas charge to the BSF in the UKSNS is thought to have been constrained by time-limited migration pathways during halokinesis in the underlying Zechstein Group and possibly during the emplacement of Tertiary dykes, resulting in underfilled traps (Underhill, 2009). Thirdly, the highest gas column is found at the Hewett Field, which lies outside of the extent of the RHM. Due to the presence of a substantive thickness of halite in the RHM, the mechanical seal capacity of the RHM is likely to exceed these empirically derived estimates, although laboratory data and *in situ* tests (such as leak-off tests) are limited.

Methodology

Mapping of halite cycles

The RHM has a characteristic response on down-hole petrophysical logs, typified by halite units with very low gamma ray (GR) values, typically less than 10 gAPI, combined with a strong positive separation of the neutron and density logs, and fast sonic velocities (Figure 4). The density log typically reads less than 2.1 g/cm^3 through the halite units while neutron porosity values are -0.05 PU. Sonic velocities are fast at 70 us/ft and generally contain little variation within the halite sections. Occasional thin shales within the halite are observed as thin GR spikes coupled with a reduction in the neutron density separation (Figure 4). In the overlying mudstone units where shales are well developed the GR log tends to read in the high 60s gAPI, while the neutron density response is opposite to that of the halite, with high neutron and density values typically 0.2 PU and 2.5 g/cm^3, respectively. The sonic velocity also slows to around 90 us/ft. All logs tend to have a spiky character reflecting the complex mineralogy of the shales and presence of minor halite and anhydrite beds within the succession.

Well-developed beds of anhydrite are occasionally present within the thick shale units, having unique density and sonic characteristics (Figure 4). Densities tend to be greater than 2.7 g/cm^3 while the sonic velocity reads fast interval velocities of 65 us/ft. The GR log response tends to trend low in these sections but can easily be overlooked as the response can be difficult to distinguish from the overall noise in the shale-dominated sections. As previously identified by Southworth (1987), thicker anhydrite units are present within the evaporite members that overlie and overstep the RHM and Upper Röt Halite. Interbedded mudstone beds have previously been used as correlative markers to sub-divide bedded Triassic halite successions elsewhere in the UK, including the Cheshire-Lancashire-Irish Sea region (Evans et al., 2011). In the UKSNS, a similar approach has allowed up to five depositional cycles to be identified that form regional correlation surfaces (Riddler, 1981;

ACCEPTED MANUSCRIPT

Downloaded from https://www.lyellcollection.org by UK Research and Innovation (UKRI/BGS/BAS) on Mar 09, 2026

Southworth, 1987). Correlation of evaporite cycles across extensive regions provides evidence of a depositional framework where similar sedimentological processes occurred basin wide.

[Figure 4]

In this study, petrophysical logs from a dataset of 600 wells were interpreted to determine the extent and thickness distribution of the individual evaporite cycles within the RHM across the UKSNS. This expanded on the earlier work of Southworth (1987). The log database was compiled from data sourced from the UK National Data Repository (https://ndr.nstauthority.co.uk/). Although detailed mapping in the Netherlands sector was not a priority of the study, a small number of wells have been incorporated to constrain mapping of RHM distribution and thickness adjacent to the Median Line maritime boundary. Log data for the Netherlands wells were obtained from the Dutch Oil and Gas Portal (https://www.nlog.nl/en), while UK onshore were obtained from British Geological Survey data holdings. In total, 28 wells were studied from the UK onshore area while 564 offshore wells were interpreted. A further eight wells from the Netherlands sector were also interrogated. Interpretation was undertaken in a systematic manner using well correlation panels predominantly comprising GR and sonic velocity (DT) logs, to identify the base of each successive cycle. Where available, additional logs such as neutron density were used to supplement the interpretation in ambiguous cases. The overlying evaporite unit, termed the Main Röt Evaporite Member (MREM) by Southworth (1987) was also interpreted, as was the underlying Röt Clay. The Dowsing Formation units above the MREM shown in Figure 3 (after Southworth, 1987), including the Upper Röt Halite Member and overlying Upper Röt Evaporite Member were also interpreted. The quality of the available digital petrophysical logs was highly variable, and logs were absent over the RHM interval for many wells. In these cases, the composite log plot image files produced by the operating companies were used to identify the marker bed depths. Illustrative cross sections demonstrating the RHM thickness variations across the study area are shown in Figure 5. Where the RHM was absent from a well, this was noted, and where possible, the probable cause of RHM absence was noted for each of these wells. A summary of the number of study wells containing RHM or where the RHM is absent is given in Table 1. A full list of wells and their classifications is provided in the supplementary material. The well correlation results were used to constrain a new RHM extent map (Figure 6), updating the extent maps shown by Cameron et al. (1992) and Heinemann et al. (2012).

[Table 1]

[Figure 5]

ACCEPTED MANUSCRIPT

Downloaded from https://www.lyellcollection.org by UK Research and Innovation (UKRI/BGS/BAS) on Mar 09, 2026

Thickness maps for individual cycles within the RHM were generated from isochore points calculated for each well, with the lateral boundaries drawn manually (Figure 7). Boundary placement was informed by thinning trends towards zero which enabled positioning of the boundary. Where no obvious thinning trend was observed from the data, the boundary was placed approximately through the midpoint between wells where the RHM cycle was present or absent and as such are expected to be a 'best-fit' approximation. Thickness grids were produced using a convergent gridding algorithm with a grid cell increment of 200 m. The isochore points were used as the primary input data source, while the evaporite cycle boundaries were assigned a thickness of zero. Exclusion of wells affected by post-depositional deformation processes (faulting, erosion, or intrusion by Zechstein evaporites) minimised anomalous bullseyes and enabled generation of depositional thickness maps. These wells are indicated and characterised by mode of deformation on Figure 6.

[Figure 6]

[Figure 7]

Complementary analyses

Petrographic analysis

Petrographic analyses can be used to complement mapping studies by providing additional insights into the depositional environment based on halite crystal morphologies. Only a single well has been identified within the study area with available core through the RHM; the 42/25d-3 CO_2 storage appraisal well, drilled at the Endurance storage site in 2013 (Figure 1). A small number of industry-acquired thin sections are available from this well in the British Geological Survey's National Geological Repository, however the sections are of poor quality as they are affected by a combination of halite lifting from the sections, air bubbles in the mounting medium and polishing artefacts. Consequently, a new polished thin section (British Geological Survey, BGS sub-sample SSK151437) was produced from the core, carefully prepared using water sensitive techniques. Although not statistically representative, the thin section was produced to provide an initial assessment of whether any additional evidence may be present to support the regional mapping and paleoenvironmental interpretation in the absence of any prior petrographic work on the formation. The section was impregnated with blue-dye epoxy resin to highlight any porosity. Optical microscopy was carried out under plane-polarized light (PPL), partial and full cross-polarized light (PXPL and XPL) conditions, using a Zeiss AxioImager A2m polarizing microscope equipped with a bespoke Zeiss AxioCam 208 digital camera. Representative images of key features were recorded in JPG format at a resolution of 3840 x 2160 pixels, using the Zeiss ZEN2 software package (Release 3.7).

Structural assessment

ACCEPTED MANUSCRIPT

Downloaded from https://www.lyellcollection.org by UK Research and Innovation (UKRI/BGS/BAS) on Mar 09, 2026

The structural configuration of the BSF and its overlying strata in the UKSNS have been described in depth by numerous CO_2 storage studies based on interpretation of seismic reflection data (Abel et al., 2025; Hollinsworth et al., 2022; Patruno et al., 2024; Williams et al., 2014). A pre-existing interpreted seismic section from Abel et al. (2025) is used here to frame a discussion on the impact of the RHM on post-depositional structural deformation of the BSF and its overlying strata. No new seismic interpretation has been conducted as part of this study. Data quality in the region is generally good, although imaging is poorer in structurally complex areas where the continuity of Triassic strata is disturbed by post-depositional mobilisation of the underlying Zechstein Group evaporites. The top and base of the RHM do not provide consistent regional seismic reflections across the UKSNS. Most regional seismic interpretations, including the study of Abel et al. (2025), interpret the top of the BSF and infer the presence of a conformable sequence of RHM above it based on the continuity of seismic character.

Review of geomechanical aspects

Halite is considered to provide an excellent top seal, both in terms of its lack of interconnected pore space (negligible permeability and capillary leakage risk in undisturbed halite) and its isotropic *in situ* stress state and ductile behaviour (low mechanical seal failure risk). Top seal potential is further enhanced by halite's ability to stream, re-anneal and re-establish lattice bonding via pressure-solution creep (Warren, 2017). Dynamic crystallisation processes such as grain boundary migration and grain size enlargement are other important deformation processes that contribute to halite's favourable top seal characteristics (Hao et al., 2023). Halite is therefore effectively self-sealing and typically exhibits very low porosities and permeabilities. While the mechanical properties of halite are clearly important to consider in any discussion on top seal efficacy, there is a relative paucity of information available from the RHM. To address this, geomechanical considerations are described by reference to the limited number of datasets and studies available within the scientific literature. The review is then discussed within the context of the RHM mapping study presented.

Results

Distribution of halite cycles

The distribution and thickness of the individual RHM cycles is shown by Figure 7. Cycle A represents the initial flooding event (Figure 7a), while Cycle B represents the most widespread deposit (Figure 7b). A stepwise decrease in depositional extent is observed from Cycle B to Cycle E. The average thickness of halite deposition follows a similar trend, with the initial Cycle A and terminating Cycle E being, on average, both the least extensive and thinnest units. Raster files for each individual cycle

ACCEPTED MANUSCRIPT

Downloaded from https://www.lyellcollection.org by UK Research and Innovation (UKRI/BGS/BAS) on Mar 09, 2026

thickness, as well as the overall thickness of the main RHM, are provided in the supplementary material.

The thickness maps (Figure 7) suggest the presence of two distinct depocentres. A northern sub-basin corresponds to the Silverpit Basin, while a southern sub-basin corresponds with the Sole Pit High and Inde Shelf, which formed prominent depocentres prior to Cimmerian uplift (Figure 1 and 2). Whilst particularly evident in the initial Cycle A, this pattern is observed to varying degrees across all cycles. The two depocentres are separated by an east to west striking feature of either non- or reduced deposition. The ubiquitous nature of this feature across the cycles may indicate that this was an area of raised topography which separated two distinct areas of accommodation space throughout deposition of the RHM. The position and strike of the feature is approximately coincident with the present day Outer Silverpit Fault Zone (Figure 1). Although the nature and structural evolution of this feature has been obscured by later mobilisation of the underlying Zechstein evaporites (Abel et al., 2025), it appears likely that an older precursor structure exerted some control on RHM deposition.

In addition to the two main depocentres, significant deposition of the RHM is also observed in the Cleveland Basin in the northwest UKSNS, with all cycles present in this area, albeit with a limited distribution of Cycle A. This suggests that the Cleveland Basin was subject to subsidence during RHM deposition, and particularly during deposition of cycles B to E (Figure 7). This supports previous studies that found the Cleveland Basin was subject to gentle thermal subsidence during the Mid. Triassic (Dixon, 1989).

Note that while the RHM is known to be present in the Netherlands sector of the Southern North Sea, the sequence has been removed beneath the Base Cretaceous Unconformity in the area immediately adjacent to the Median Line boundary.

Controls on deposition

It is believed that all cycles were deposited at or close to sea level, hence while the cyclicity was driven by eustatic sea level changes, the RHM thickness variations should be representative of structural movements and evolving accommodation in the basin during deposition (Southworth, 1987). The cyclicity itself resulted from comparatively minor eustatic sea level changes that mirrored on a smaller scale the larger eustatic cycles observed in the wider SPB throughout the Middle to Late Triassic. A plausible route for flooding can be observed in all cycles (Figure 7). A connection to the wider SPB was established to the north of the Cleaver Bank High, enabling flooding of the northern depocentre (Figure 7f). Initial flooding of the southern depocentre was enabled by a connection between the two depocentres located close to the junction between the Dowsing Fault Zone and the

ACCEPTED MANUSCRIPT

Downloaded from https://www.lyellcollection.org by UK Research and Innovation (UKRI/BGS/BAS) on Mar 09, 2026

precursor faults underlying the present-day Outer Silverpit Fault Zone (Figure 7f). The asymmetrical distribution of the individual halite cycles (Figure 7) further supports this interpretation, indicating a rapid sea level rise followed by a more gradual lowering of the base level.

Several authors have previously postulated that the extent and thickness distributions of the RHM cycles were controlled by passive depressions on the underlying Hardegsen Unconformity surface, which subsequently became less pronounced over time as the topography was filled by evaporite deposition (Fisher, 1984; Harsveldt, 1978; Ziegler, 1975). In contrast, Southworth (1987) proposed that rapidly subsiding active structural lows (e.g. the Sole Pit Trough) exerted the principal influence. The correlation of the cycle thickness distributions with regional structural maps (Figure 1; Figure 7) supports this latter interpretation. This is particularly relevant for Cycle A, which would otherwise be expected to be most influenced by passive depressions in the substratum. However, it arguably exhibits the clearest relationship to regional tectonic structures (Figure 7).

The western and southern extent of the RHM appear to be constrained by depositional processes rather than by subsequent uplift and removal or dissolution. Evidence for this is seen by the gradual thinning of the RHM towards the margins of the salt basin together with the presence of the contemporaneous marginal and overstepping facies of the Main Röt Evaporite. Taken together, these observations are suggestive of subsidence in the active depocentres driving the availability of accommodation space. There is a paucity of wells with which to constrain the distribution and thickness maps towards the northern extent of the RHM. Regardless, it is postulated that the Mid North Sea High would have presented a positive feature that limited the northern extent of the RHM. Significant uplift on the margins of the Cleaver Bank High has led to removal of much of the Jurassic and Triassic strata beneath the Base Cretaceous Unconformity. Consequently, the RHM has been entirely removed in some wells. However, a fringe of the Main Röt Evaporite is preserved along the margins of the Cleaver Bank High, suggesting that structural elevation would have constrained this eastern margin, with gradual thinning of the RHM prior to gradation to marginal sabkha facies. Absence of RHM in this area must therefore relate to lack of deposition rather than post-depositional erosion beneath the Base Cretaceous Unconformity. This is illustrated by the schematic geological section in Figure 8, which shows both the depositional transition from halite to marginal facies of the Main Röt Evaporite unit and the progressive downcutting of the Base Cretaceous Unconformity eastwards onto the Cleaver Bank High. Similarly, the presence of Lower Cretaceous strata directly above Lower Triassic Bacton Group sediments in the Netherlands sector wells adjacent to the northeastern extent of the UKSNS indicate post-depositional removal of the RHM related to Cimmerian uplift (Figure 2). Evidence of the postulated connection between the Netherlands and UK

ACCEPTED MANUSCRIPT

Downloaded from https://www.lyellcollection.org by UK Research and Innovation (UKRI/BGS/BAS) on Mar 09, 2026

sectors of the Southern North Sea in this area shown in Figure 7f, that would have enabled flooding of the UKSNS and deposition of the RHM, has therefore been removed during this erosional event.

[Figure 8]

Depositional environment

Accumulation of bedded halite gives rise to a suite of characteristic fabrics that can be related to primary crystal development. In a study of experimentally produced halite (Arthurton, 1973), it was shown that some distinctive fabrics, including elongate chevron-shaped crystals, can be associated with the primary accumulation of halite. These are postulated to develop upwards due to the competitive growth of crystals from foundered mats of halite at the base of a brine-pan (Arthurton, 1973). Crystals with this distinctive chevron form were observed in the BGS thin section, sampled from Cycle B in the 42/25d-3 CO_2 storage appraisal well at the Endurance site (Figure 9). Fluid inclusions are present in dense patches, delineating the outline of euhedral cubic halite and chevron halite. These forms are indicative of primary, bottom-crystal growth in a marginal marine setting. However, the current crystallographic boundaries do not correspond to the crystal morphology defined by the dense patches of fluid inclusions. This indicates that the halite in this thin section has been completely recrystallised since deposition (a common observation in halite deposits), and that the current crystal boundaries are secondary.

[Figure 9]

The preservation of crystal forms that indicate a primary bedded origin is relevant to understanding the accumulation of the RHM. This crystal form and fabric will only develop in shallow brines (e.g., approximately 5 m) where brine stratification has not led to the formation of different suites of crystals (e.g., cumulate facies). The correlation of relatively uniform halite units observed from log data over distances exceeding 100 km indicates that similar depositional conditions may have been contiguous over large parts of the basin, allowing the penecontemporaneous accumulation of halite beds. Mudstone accumulation was probably initiated during times when brine replenishment to the basin had been cut-off, restricting the amount of halite that could crystallise. Given the strong cyclicity in halite-mudstone deposition over such an extensive area, it is likely that these cycles developed in response to a regional climatic control with strong seasonality (e.g., Kutzbach and Gallimore, 1989; Newell, 2018; Milroy et al., 2019; Ruffel and Kurschner, 2020). Additional sections would be required to investigate formation fabrics further, and to validate the interpretation presented. However, it is noteworthy that such evidence is apparent from a single sample. This suggests further petrographic study would be worth consideration during future appraisal activities for CO_2 storage.

ACCEPTED MANUSCRIPT

Downloaded from https://www.lyellcollection.org by UK Research and Innovation (UKRI/BGS/BAS) on Mar 09, 2026

Implications for top seal

Halite thickness and continuity

Correlation of petrophysical logs suggest a conformable and generally uninterrupted distribution of the RHM across the basin. This may suggest a shallow brine pan environment, as inferred from optical microscopy, was prevalent over extensive regions, particularly during the deposition of RHM Cycles B to D. This would imply that the top seal character is likely to be consistent across the extent of the RHM, particularly in areas where the thickest halite units were developed (Figure 10). Despite this, it is important to note that the petrographic analysis in this study is limited to a single sample and caution should be exercised in extrapolating the interpretation. The lack of core material from the RHM across the basin is a major constraint, and analysis of future borehole material would help calibrate the lateral extents of depositional conditions and sedimentary character of the RHM across the basin, whilst also enabling quantifiable capillary and mechanical seal evaluations.

A map detailing the number of RHM cycles across the UKSNS is shown in Figure 11, overlain with current carbon storage licence blocks. This was generated by overlaying and stacking the extent polygons for each RHM cycle, therefore illustrating both the cycle number in each area, as well as marking the areas where cycle margins are inferred. The margins of each cycle are relevant to seal integrity studies for two reasons. Firstly, halite may possibly have been subject to dissolution processes, which could potentially have resulted in deformation and fracturing which are known to form seal bypass systems through salt (Cartwright et al., 2007). Secondly, the presence of impurities such as shale or carbonate may render the halite locally porous or brittle. The Main Röt Evaporite unit provides an example of a contemporaneous transition from halite to basin margin facies. Second-phase materials within rock salt, specifically anhydrite, can reduce strength by creating planes of weakness or facilitating certain deformation mechanisms at lower stress (Martin-Clave et al., 2021). Further to this, they may also act as migration pathways by forming interconnected networks along grain boundaries which can potentially act as preferential fluid flow pathways (Zhang et al., 2020). While these risks may be considered relatively low or even negligible within the overall context of a containment risk assessment, the location of such margins may be used to identify objectives for further appraisal and risk reduction measures. This risk would be mitigated to some extent where the RHM evaporite cycles are overstepped by subsequent cycles, such as where Cycle B oversteps Cycle A. However, cycles C to E represent a stepwise contraction of the evaporite basin (Figure 7). Therefore, the most effective top seal potential is likely to exist where the thickest cycles B, C and D are present, which also corresponds to the thickest total accumulation of RHM with a mean thickness of 55 m. It is worth noting that except where removed beneath the Base Cretaceous Unconformity, a significant thickness of overlying Haisborough Group strata are present above the

ACCEPTED MANUSCRIPT

Downloaded from https://www.lyellcollection.org by UK Research and Innovation (UKRI/BGS/BAS) on Mar 09, 2026

RHM across most of the basin. Given the lithological composition of the Haisborough Group (playa, estuarine and loessic mudstone, coastal sabkha and marine evaporite deposits), lack of RHM at a given location does not preclude the presence of a potentially effective top seal succession.

[Figure 10]

[Figure 11]

The location of wells where the continuity of the RHM has been interrupted by post-depositional processes, resulting in degradation of the top seal, are shown (Figure 10). These include wells where the sequence is absent due to localised faulting, where the RHM has been intruded by mobile Zechstein evaporites, or eroded, for example due to Cimmerian uplift and erosion. Figure 12 shows a seismic reflection line illustrating the role of the RHM in controlling the post-depositional deformation processes affecting the BSF and its top seal succession. Zones of significant deformation and halokinesis are largely constrained to major structural discontinuities caused by post-depositional mobility of underlying evaporites of the Zechstein Group (Figure 12). At these major fault zones, the RHM is also prone to invasion by mobile potassium-rich Zechstein salts resulting in thick allochthonous salt bodies overhanging the BSF. This is observed at the Outer Silverpit Fault Zone, where faults completely offset and laterally dislocate the Bacton Group (Figure 12a). Structures such as these where thick allochthonous salt bodies overhang the BSF (i.e. Figure 12a) could provide attractive options for CO_2 storage if they could be suitably de-risked. However, in the example shown (Figure 12a), lack of structural closure may preclude the selection of such sites for CO_2 storage.

[Figure 12]

Role of faults

Pre-existing faults represent one of the key geological containment uncertainties for carbon dioxide storage in the BSF (Williams et al., 2014). Many of the structural closures of interest for CO_2 storage in the UKSNS are affected by extensional faults associated with folding during formation of the structural closures. Faults are particularly evident over the crests of structures and on the flanks (Figure 12), where post-Triassic tectonic activity and halokinesis has resulted in abundant faulting of the overburden (Williams et al., 2014; Hollinsworth et al., 2022). The Bacton Group, which comprises the BSF, is bounded by the Zechstein evaporites below and the RHM above, allowing for mechanical decoupling from older Carboniferous and Permian strata below, and the Middle Triassic and younger strata above (Van Hoorn, 1987; Stewart and Coward, 1995, Abel et al., 2025). This decoupling results in buckling of the Bacton Group and isolation from the brittle deformation seen in the overburden.

ACCEPTED MANUSCRIPT

Downloaded from https://www.lyellcollection.org by UK Research and Innovation (UKRI/BGS/BAS) on Mar 09, 2026

Characterisation activities at the Endurance storage site indicate that the RHM plays an important role as a décollement horizon, commonly preventing faults in the overburden from penetrating downwards through the RHM and into the BSF (Gibson-Poole et al., 2024). Elsewhere in the UKSNS, these crestal faults have been shown to offset the top BSF (Bentham et al., 2013; Williams et al., 2014). While several structures are affected by small-offset crestal faults that are often close to the resolution of conventional seismic reflection data, fault throw is sufficient to fully displace the BSF at some locations.

Figure 12 shows some of the differing degrees of deformation within the BSF in contrast with its overburden. Small offset faults penetrate the RHM and offset the BSF in Figure 12b. However, many of the faults terminate in the RHM above the Bacton Group with enhanced throws clearly observed at top Triassic level. The Top Bacton Group (top BSF) reflector is less consistent over the crest of the anticline (Figure 12b), which may be in part due to the complexity of the faulting and the mechanical response of the RHM. Some uncertainty as to how the RHM influences the geometry of the faults at the RHM-BSF interface remains due to the limited resolution of the seismic data. The northernmost anticline (Figure 12c) is affected by extensional faulting on the southern flank, a similar structural style observed at some other anticlinal structures in the UKSNS. Here the RHM provides a slip surface resulting in gravitational slumping towards the south. Whilst the imaging of the seismic data is relatively poor, this slumping may have potentially led to mobilisation of the RHM, causing it to intrude along the fault planes. Such salt redistribution may locally reduce RHM thickness or remove it entirely, causing the formation of salt welds.

The UK's digital CO_2 storage atlas, CO_2Stored (Bentham et al., 2013, 2014), contains qualitative fault risk ratings for BSF structures identified for potential CO_2 storage. A preliminary assessment was conducted to identify if the density and throw of faults affecting the BSF structures had any relationship to the RHM thickness distribution or number of evaporite cycles present (Figure 13). No obvious relationships were observed, suggesting that numerous site-specific factors related to the geological evolution of each structure controls the extent to which overburden faults extend downwards through the RHM and into the BSF. Where present, the RHM may reduce the risk of vertical migration along any faults due to the ability of halite to reseal by combination of flow and pressure solution creep (Warren, 2016).

[Figure 13]

Geomechanical considerations

ACCEPTED MANUSCRIPT

Downloaded from https://www.lyellcollection.org by UK Research and Innovation (UKRI/BGS/BAS) on Mar 09, 2026

In the UKSNS, very few data are available with which to characterise the geomechanical integrity of the RHM, although creep data derived from a laboratory analysis has confirmed the expected non-linear viscous/plastic behaviour (National Grid, 2016). A single Formation Integrity Test (FIT) pressure taken at the 9⅝ inch casing shoe in the 42/25d-3 well at Endurance, measured an equivalent mud weight of 22 MPa at approximately 1340 m sub-sea depth. This compares to the estimated fracture pressure for the UKSNS of 22.6 MPa as calculated using the gradients presented by Noy et al. (2012). Although the FIT value does not reflect the formation fracture pressure, it indicates that the RHM is capable of withstanding pressures at least as high as this value without fracturing. In practice a greater fracture pressure equal to the lithostatic stress would be expected. Again, using the gradients presented by Noy et al. (2012), it would be expected that the lithostatic stress at a depth of 1340 m would be in the region of 30 MPa. Near the boundaries of the evaporite cycles, as shown in Figures 7 and 11, the RHM is more likely to consist of impure halite or other more brittle lithologies. Consequently, it is possible that the mechanical integrity of the RHM might be locally reduced in these regions.

Cooling-related stresses may pose a potential risk to seal integrity given that injected CO_2 is likely to be significantly cooler than the ambient temperature of the subsurface. Relative to most rocks, halite has an approximately three times greater Linear Thermal Expansion Coefficient (LTEC) of 4x10-5/℃ at relevant temperatures of between 20 and 60℃ (National Grid, 2016). This means that halite is more susceptible to greater axial strain due to changes in temperature. Added to this, halite may exhibit reduced ductility at lower temperatures, increasing the risk of brittle failure rather than ductile crystal plastic recrystallisation (Chester, 1988; Borthwick and Piazolo, 2010). Regional simulation of CO_2 storage scenarios in the BSF indicates that the cooling effect is restricted to a c. 800 m radius around the injection wells, within which the RHM would experience contractional strain (Williams et al., submitted this volume). This was identified as a potential risk in previous geomechanical modelling studies of the BSF (National Grid, 2016; ETI, 2016). Suggested mitigations included perforation and injection into the lower part of the BSF succession as a means of minimising the cooling effect at the interface between the reservoir and top seal (ETI, 2016). The presence of any low-permeability barriers or baffles within the reservoir would impede upward migration of the cold CO_2 plume and act to minimise cooling of the RHM. Risk of thermal fracture is likely to be reduced in regions where the RHM is thickest, such as the centre of the Silverpit Basin and northern parts of the Inde Shelf and Sole Pit High (Figures 1 and 10). Nevertheless, it is recommended that thermal stress effects are carefully considered during coupled flow and geomechanical modelling for potential CO_2 storage sites where the RHM forms a top seal for the BSF.

ACCEPTED MANUSCRIPT

Downloaded from https://www.lyellcollection.org by UK Research and Innovation (UKRI/BGS/BAS) on Mar 09, 2026

Insights into the creep behaviour of the RHM have been observed during decommissioning of the Schooner Gas Field, a field with reservoirs of Carboniferous age in the Silverpit Basin region. A key objective of the well abandonment process was the qualification of the abandonment barriers in the overlying BSF to the maximum pressure expected during future CO_2 storage operations in the BSF (Loizzo et al., 2024). The thickness range of the RHM over the field is approximately 50–60 m. For a large proportion of legacy wells in the UKSNS, isolation of the BSF was not a primary objective during well design and construction. Consequently, understanding the interaction of the RHM with wells with poor or absent cement is an important consideration for CO_2 storage projects in the BSF. A comprehensive abandonment logging and testing programme showed that the creep behaviour of the RHM contributes positively to barrier qualification (Loizzo et al., 2024). However, the presence of carnallite in the RHM was inferred from log inversion results during abandonment logging. Carnallite has a lower pressure rating than halite, and pressure can therefore more easily exceed the radial stress at the rock-casing interface leading to potential de-bonding and creation of microannuli (Loizzo et al., 2024). When coupled with the higher solubility of carnallite, where present, the effectiveness of the RHM as an effective barrier element could be reduced. For these reasons, specific care may be required during drilling and well construction through the RHM to ensure preservation of the well barrier for CO_2 storage operations (Loizzo et al., 2024). X-Ray Diffraction (XRD) data reported from a single core sample at Endurance indicates a mineralogical content of 99.7% halite and 0.3% anhydrite, with no indications of carnallite (Blackbourn and Robertson, 2014). Due to the lack of further sample material and associated analytical data it is not clear how representative this is of the mineralogical content of the RHM across the UKSNS. The conflicting information on the presence of carnallite, albeit from a small number of samples and locations, indicates that a comprehensive assessment of the mineralogical content of the RHM is required to identify if non-halite phases such as carnallite are present. Carnallite is commonly formed in hypersaline environments, typically forming in the upper layers of salt deposits once brine becomes highly concentrated with potassium and magnesium ions following halite precipitation. It is possible that it might be present elsewhere in the RHM of the UKSNS where it is most likely to be found near the top of the individual halite units. It has been identified onshore in Permian evaporite sequences along with other Magnesium salts (Armstrong et al., 1951). Acquisition and preservation of physical RHM samples suitable for detailed mineralogical analyses is recommended during CO_2 storage appraisal drilling to ascertain if non-halite mineral phases are present, and the degree to which they are distributed throughout the RHM sequence.

ACCEPTED MANUSCRIPT

Downloaded from https://www.lyellcollection.org by UK Research and Innovation (UKRI/BGS/BAS) on Mar 09, 2026

Conclusions

The detailed well log data accumulated in this study have been used to synthesise a series of stratigraphic and depositional interpretations for the RHM in the UKSNS, building on and enhancing previous work in the region. The primary aim was to better characterise the thickness and extent of the cyclical sub-units that form the RHM, and to discuss the implications with respect to the RHM as a top seal for CO_2 storage. We also integrate this analysis with further information derived from petrographic analysis, structural insights from reflection seismic observations and a review of geomechanical considerations and available datasets. The results can be used to better inform CO_2 storage developments seeking to exploit the properties of the RHM as a top seal for CO_2 storage in the underlying BSF, by providing a regional framework and context for characterisation of the RHM.

The log interpretations allowed for the creation of thickness and extent maps for the five identified evaporite cycles in the RHM, providing an understanding of the evolution of the RHM evaporite basin and controls on deposition. A key feature includes the presence of two main depocentres active throughout RHM deposition. The northern depocentre corresponds with the Silverpit and Cleveland basins, while the second depocentre to the south, corresponds to the present-day Sole Pit High and Inde Shelf. The western and southern extent of the RHM appears to represent the depositional limit, evidenced by the thinning of cycles towards the basin margins and the presence of marginal facies of the Main Röt Evaporite. This suggests that subsidence was active during RHM deposition, driving the creation of accommodation space along with active syn-depositional movement on pre-existing structures such as the Dowsing Fault Zone. In the eastern part of the study area on the flanks of the Cleaver Bank High, the mapping illustrates a similar trend of thinning cycles and overstepping of the Main Röt Evaporite. This indicates that the Cleaver Bank High had positive relief throughout deposition of the RHM. Although well data are scarce in the northern part of the UKSNS, the Mid North Sea High is inferred to have similarly provided structural relief which constrained the northern extent of the RHM. It is interpreted that the UKSNS basin was connected at this time to the Netherlands sector in the northeast of the study region, via a topographic low between the Mid North Sea High to the north and the Cleaver Bank High to the south. This would have enabled the ingress of marine waters into the UKSNS leading to deposition of the RHM (Figure 7f). Physical evidence for a direct connection between the RHM in the UKSNS and the wider SPB to the east has been removed due to post-depositional uplift and erosion of Triassic strata beneath the Base Cretaceous Unconformity.

Analysis of a thin section sample from RHM Cycle B provided supporting evidence into the possible depositional environment. Core availability throughout the RHM is scarce, with only an incomplete

ACCEPTED MANUSCRIPT

Downloaded from https://www.lyellcollection.org by UK Research and Innovation (UKRI/BGS/BAS) on Mar 09, 2026

section of core acquired from the 42/25d-3 CO_2 storage appraisal well from Endurance being known to the authors. Evidence recorded in the thin section of primary crystal morphologies and fabric indicate that the depositional environment consisted of shallow brine pans, as the absence of cumulate or other crystal suites indicates a lack of brine stratification. The implication of the regional mapping results is that this shallow subaqueous depositional environment was prevalent over very large areas, with a relatively flat substratum allowing for extensive and relatively uninterrupted brine pan development and halite deposition. The lateral continuity of the halite units provides assurance from a top seal perspective given the excellent proven sealing capacity of halite. A key observation of the study is that limited data are available with which to characterise the petrographic properties of the RHM. Intact core material is limited to a partial section from a single well and limited quantitative and descriptive characterisation has been undertaken to date. Further sampling of the RHM is recommended during CO_2 storage appraisal to enhance the sparse petrographic database and to gain a more complete understanding of the mineralogical content of the RHM.

The RHM has been identified as a potential décollement horizon, preventing overburden faults from extending downwards into the BSF over some structures (Williams et al., 2014; Gibson-Poole et al., 2024). Conversely, in some cases the presence of the RHM combined with steep angles of structural dip generated during post-depositional halokinesis (in the underlying Zechstein Group), has resulted in gravitational slumping of overlying strata (Abel et al., 2025). This may have initiated mobilisation of the RHM along fault planes, resulting in locally variable RHM thickness in affected areas (i.e. Figure 12c). To evaluate the impact of RHM thickness on post-depositional faulting, the depositional thickness maps generated in this study were compared against risk ratings for fault density and displacement applied to the underlying BSF structural closures in the CO_2Stored storage atlas (Bentham et al., 2014). No simple relationships were observed between RHM thickness and number of individual evaporite cycles relative to the qualitative measures of fault density and throw available from the CO_2Stored database. This implies that the RHM thickness and number of depositional cycles cannot be used as predictive measures to infer likelihood of fault density or throw affecting the underlying BSF storage target.

The understanding presented here provides a regionally applicable framework with which to consider the RHM in relation to CO_2 containment risk. In broad terms, where present the RHM is expected to provide an effective top seal for CO_2 storage sites in the BSF. Detailed correlation of the cyclicity within the RHM across the extent of the UKSNS indicates a setting in which consistent evaporite cycles were deposited across extensive regions. Top seal quality is likely to be enhanced where the more extensive cycles B, C, and D are present, which corresponds to the thickest parts of the RHM. Cycle boundaries, particularly where multiple cycle terminations are co-located in narrow

ACCEPTED MANUSCRIPT

Downloaded from https://www.lyellcollection.org by UK Research and Innovation (UKRI/BGS/BAS) on Mar 09, 2026

zones, may require further assessment to ensure that the top seal potential is not negatively impacted by enhanced presence of relatively brittle non-halite rocks, fractures, or dissolution features.

Acknowledgements

We acknowledge funding from the UK Carbon Capture and Storage Research Centre 2017 (EPSRC Grant EP/P026214/1), the Industrial Decarbonisation Research and Innovation Centre (EPSRC Grant EP/V027050/1), and the Managing the Environmental Sustainability of the Offshore Energy Transition (MOET) project, funded by the NERC National Capability Multi-Centre Science programme. British Geological Survey National Capability funding from NERC is also gratefully acknowledged. SLB are thanked for provision of Petrel software licences. This paper is published with the permission of the Executive Director, British Geological Survey (NERC, UKRI).

References

Abel, L., Williams, J.D.O., Wright, K., Randles, T., Bridger, P., Morris, H.A., Dodd, T., Plenderleith, G. and White, J.C. 2025. Structural controls on pressure communication across the Bunter Sandstone Formation, UK Southern North Sea. Geoenergy, 3, geoenergy2024-027. https://doi.org/10.1144/geoenergy2024-027

Agada, S., Jackson, S., Kolster, C., MacDowell, N., Williams, G., Vosper, H., Williams, J. and Krevor, S. 2017. The impact of energy systems demands on pressure limited CO_2 storage in the Bunter Sandstone of the UK Southern North Sea. International Journal of Greenhouse Gas Control, 65, 128–136. https://doi.org/10.1016/j.ijggc.2017.08.014

Allen, M.R., Griffiths, P.A., Craig, J., Fitches, W.R. and Whittington, R.J. 1994. Halokinetic initiation of Mesozoic tectonics in the southern North Sea: A regional model. Geological Magazine, 131, 559–561. https://doi.org/10.1017/S0016756800012164

Armitage, P.J., Worden, R.H., Faulkner, D.H., Aplin, A.C., Butcher, A.R. and Espie, A.A. 2013. Mercia Mudstone Formation caprock to carbon capture and storage sites: petrology and petrophysical characteristics. Journal of the Geoloigcal Society, London, 170, 119–132. https://doi.org/10.1144/jgs2012-049

Armstrong, G., Dunham, K.C., Harvey, C.O., Sabine, P.A. and Waters, W.F. 1951. The paragenesis of sylvine, carnallite, polyhalite, and kieserite in eskdale borings nos. 3, 4, and 6, north-east yorkshire. Mineralogical Magazine and Journal of the Mineralogical Society, 29 (214), 667–689. doi:10.1180/minmag.1951.029.214.02

ACCEPTED MANUSCRIPT

Downloaded from https://www.lyellcollection.org by UK Research and Innovation (UKRI/BGS/BAS) on Mar 09, 2026

Arthurton, R.S. 1973. Experimentally produced halite compared with Triassic layered halite-rock from Cheshire, England. Sedimentology, 20, 145–160. https://doi.org/10.1111/j.1365-3091.1973.tb01611.x

OPC. 2011. Offshore Petroleum and Greenhouse Gas Storage (Greenhouse Gas Injection and Storage) Regulations 2011. Select Legislative Instrument 2011 No. 107. Australia Office of Parliamentary Council. Available at https://classic.austlii.edu.au/cgi-bin/download.cgi/au/legis/cth/num_reg_es/opaggsgiasr2011n107o2011953

Bentham, M., Williams, G., Vosper, H., Chadwick, A., Williams, J. and Kirk, K. 2017. Using pressure recovery at a depleted gas field to understand saline aquifer connectivity. Energy Procedia, 114, 2906–2920. https://doi.org/10.1016/j.egypro.2017.03.1418

Bentham, M.S., Green, A. and Gammer, D. 2013. The occurrence of faults in the Bunter Sandstone of the UK sector of the Southern North Sea and the potential impact on storage capacity. Energy Procedia, 37, 5101–5109. https://doi.org/10.1016/j.egypro.2013.06.423

Bentham, M., Mallows, T., Lowndes, J. and Green, A. 2014. CO_2 STORage Evaluation Database (CO_2 Stored). The UK's online storage atlas. Energy Procedia, 63, 5103–5113. https://doi.org/10.1016/j.egypro.2014.11.540

Blackbourn, G.A. and Robertson, L.F. 2014. Sedimentology, Petrography and Burial History of the Cored Triassic Section in the National Grid Carbon Well 42/25d-3, UK North Sea. Blackbourn Geoconsulting, Bo'ness, West Lothian, UK. Available at https://ndr.ogauthority.co.uk/

Borthwick, V.E. and Piazolo, S. 2010. Post-deformational annealing at the subgrain scale: Temperature dependent behaviour revealed by in-situ heating experiments on deformed single crystal halite. Journal of Structural Geology, 32 (7), 982–996. https://doi.org/10.1016/j.jsg.2010.06.006

Brackenridge, R.E., Underhill, J.R., Jamieson, R. and Bell, A. 2020. Structural and stratigraphic evolution of the Mid North Sea High region of the UK Continental Shelf. Petroleum Geoscience, 26, 154–173. https://doi.org/10.1144/petgeo2019-076

Cameron, T.D.J., Crosby, A., Balson, P.S., Jeffery, D.H., Lott, G.K., Bulat, J., and Harrison, D.J. 1992. The Geology of the Southern North Sea. United Kingdom Offshore Regional Report, British Geological Survey and HMSO, London.

Cartwright, J., Huuse, M. & Aplin, A. 2007. Seal bypass systems. AAPG Bulletin, 91, 1141–1166. https://doi.org/10.1306/04090705181

ACCEPTED MANUSCRIPT

Downloaded from https://www.lyellcollection.org by UK Research and Innovation (UKRI/BGS/BAS) on Mar 09, 2026

Chester, F.M. 1988. The brittle-ductile transition in a deformation-mechanism map for halite. Tectonophysics, 154 (1–2), 125–136. https://doi.org/10.1016/0040-1951(88)90230-2

Davis, J.S., Jonk, R. and Bohacs, K.M. 2024. Evaluating CO_2 retention risk of geological sequestration sites: physical, time-scale, and site style considerations. Geoenergy, 2, geoenergy2024-009. https://doi.org/10.1144/geoenergy2024-009

Davison, I. 2009. Faulting and fluid flow through salt. Journal of the Geological Society, London, 166, 205–216. https://doi.org/10.1144/0016-76492008-064

de Jonge-Anderson, I., Hollinsworth, A.D., Underhill, J.R. and Jamieson, R.J. 2022. A geological assessment of the carbon storage potential of structural closures in the East Midlands shelf, United Kingdom Southern North Sea. AAPG Bulletin, 106 (9), 1827–1853. https://doi.org/10.1306/03232221118

Dixon, A.D.G. 1989. Evolution of the Yorkshire, sole pit and east midland basin system, U.K. PhD thesis, Durham University. Available at Durham E-Theses Online: http://etheses.dur.ac.uk/6695/

Doornenbal, H., and Stevenson, A. (Eds.) 2010. Petroleum Geological Atlas of the Southern Permian Basin Area. EAGE, Houten, The Netherlands. Available at https://www.nlog.nl/southern-permian-basin-atlas

EC. 2009. Directive 2009/31/EC of the European Parliament and of the Council of 23 April 2009 On the Geological Storage of Carbon Dioxide and Amending Council Directive 85/337/EEC, European Parliament and Council Directives 2000/60/EC, 2001/80/EC, 2004/35/EC, 2006/12/EC, 2008/1/EC and Regulation (EC) No 1013/ 2006 (Text With EEA Relevance). https://eur-lex.europa.eu/legal-content/EN/TX T/?uri=CELEX%3A32009L0031.

ETI. 2016. D10: WP5A – Bunter Storage Development Plan 10113ETIS-Rep-13-03, March 2016. Available at https://ukerc.rl.ac.uk/ETI/PUBLICATIONS/CCS_CC1026_8.pdf

Evans, D.J. and Holloway, S. 2009. A review of onshore UK salt deposits and their potential for underground gas storage. In: Evans, D.J. and Chadwick, R.A. (Eds.). Underground Gas Storage: Worldwide Experience and Future Development in the UK and Europe. Geological Society, London, Special Publications, 313, 39–80.

Evans, D.J., Williams, J.D.O. and Hough, E. 2011. The stratigraphy and lateral correlations of the Northwich and Preesall halites from the Cheshire Basin-East Irish Sea areas: implications for sedimentary environments, rates of deposition and the solution mining of gas storage caverns. Solution Mining Research Institute Technical Conference Paper, SMRI Fall 2011 Technical Conference,

ACCEPTED MANUSCRIPT

Downloaded from https://www.lyellcollection.org by UK Research and Innovation (UKRI/BGS/BAS) on Mar 09, 2026

York, England, 2–4 October 2011. MP2011F-2011. https://nora.nerc.ac.uk/id/eprint/15562/1/Evans_et_al_SMRI_MP2011F_2011.pdf

Fisher, M. J. 1984. Triassic. In: Glennie, K.W. (Ed.), Introduction to the Petroleum Geology of the North Sea, Blackwell Scientific Publications, 85–102.

Furnival, S., Wright, S., Dingwall, S., Bailey, P., Brown, A., Morrison, D. and De Silva, R. 2014. Subsurface Characterisation of a Saline Aquifer Cited for Commercial Scale CO_2 Disposal. Energy Procedia, 63, 4926–4936. https://doi.org/10.1016/j.egypro.2014.11.523

Geluk, M.C. 2005. Stratigraphy and tectonics of Permo-Triassic basins in the Netherlands and surrounding areas. PhD thesis, Utrecht University. Available at https://dspace.library.uu.nl/handle/1874/1699

Geluk, M.C. and Röhling, H.-G. 1997. High-resolution sequence stratigraphy of the Lower Triassic 'Buntsandstein' in the Netherlands and northwestern Germany. Geologie en Mijnbouw, 76, 227–246. https://doi.org/10.1023/A:1003062521373

Gibson-Poole, C.M., Taplin, M., Bouffin, N., Duffy, L., Sutherland, F., Cabral, A. and Ashby, D. 2024. Site Characterization of the Endurance CO_2 Store, Southern North Sea, UK. Geoenergy, 2, 2024-012. https://doi.org/10.1144/geoenergy2024-012

Glennie, K.W. 1990. Outline of North Sea history and structural framework. In: Glennie K.W (Ed.), Introduction to the Petroleum Geology of the North Sea. Blackwell Scientific Publications, Oxford, 34–77.

Gluyas, J.G. and Bagudu, U. 2020. The Endurance CO_2 storage site, Blocks 42/25 and 43/21, UK North Sea. In: Goffey, G. and Gluyas, J.G. (Eds.), United Kingdom oil and gas fields: 50th anniversary commemorative volume. Geological Society, London, Memoirs, 50, 163–171. https://doi.org/10.1144/M52-2019-47

Grant, R.J., Underhill, J.R., Hernández-Casado, J., Jamieson, R.J. and Williams, R.M. 2019. The evolution of the dowsing graben system: Implications for petroleum prospectivity in the UK Southern North Sea. Petroleum Geoscience, 27, petgeo2018-064. https://doi.org/10.1144/petgeo2018-064

Grant, R.J., Booth, M.G., Underhill, J.R. and Bell, A. 2020. Structural evolution of the Breagh area: implications for carboniferous prospectivity of the Mid North Sea High, Southern North Sea. Petroleum Geoscience, 26, 174–203. https://doi.org/10.1144/petgeo2019-10

Griffiths, P.A. Allen, M.R., Craig, J., Fitches, W.R. and Whittington, R.J. 1995. Distinction between fault and salt control of Mesozoic sedimentation on the southern margin of the Mid-North Sea High. In:

ACCEPTED MANUSCRIPT

Downloaded from https://www.lyellcollection.org by UK Research and Innovation (UKRI/BGS/BAS) on Mar 09, 2026

Boldy, S.A.R. (Ed.), Permian and Triassic Rifting in Northwest Europe. Geological Society, London, Special Publications, 91, 145–159. https://doi.org/10.1144/GSL.SP.1995.091.01.08

Hannis, S., Bricker, S., Goater, A., Holloway, S., Rushton, J., Williams, G. and Williams, J. 2013. Cross-international boundary effects of CO_2 injection. Energy Procedia, 37, 4927–4936. https://doi.org/10.1016/j.egypro.2013.06.404

Hao, B., Llorens, M-G.,Griera, A., Bons, P.D., Lebensohn, R.A., Yu, Y. and Gomez-Rivas, E. 2023. JGR Solid Earth, 128 (12), e2023JB027590. https://doi.org/10.1029/2023JB027590

Harsveldt, H.M. 1978. Salt resources in the Netherlands as surveyed mainly by AKZO. In: Coogan, A.H. and Hauber, L. (Eds.), Fifth International Symposium on Salt, Vol. 1. The Northern Ohio Geological Society, Inc. Cleveland. 65–81

Haq, B.U., Hardenbol, J. and Vail, P.R. 1987. Chronology of Fluctuating Sea Levels Since the Triassic. Science, 235, 1156–1167. DOI: 10.1126/science.235.4793.1156

Heinemann, N., Wilkinson, M., Pickup, G.E., Haszeldine, R.S. and Cutler, N.A. 2012. CO_2 storage in the offshore UK Bunter Sandstone Formation. International Journal of Greenhouse Gas Control, 6, 210–219. https://doi.org/10.1016/j.ijggc.2011.11.002

HMSO. 2010. The Storage of Carbon Dioxide (Licensing etc.) Regulations 2010. His Majesty's Stationary Office. Available at https://www.legislation.gov.uk/uksi/2010/2221/contents

Hollinsworth, A.D., de Jonge-Anderson, I., Underhill, J.R. and Jamieson, R.J. 2022. Geological evaluation of suprasalt carbon storage opportunities in the Silverpit Basin, United Kingdom Southern North Sea. AAPG Bulletin, 106, 1791–1825. https://doi.org/10.1306/03232221119

Hollinsworth, A.D., de Jonge-Anderson, I., Underhill, J.R. and Jamieson, R.J. 2024. Impact of reservoir quality on the carbon storage potential of the Bunter Sandstone Formation, Southern North Sea. Geoenergy, 2, 2023-037. https://doi.org/10.1144/geoenergy2023-037

Holloway, S., Vincent, C.J., Bentham, M.S. and Kirk, K.L. 2006. Top-down and bottom-up estimates of CO_2 storage capacity in the UK sector of the Southern North Sea Basin. Environmental Geoscience, 13, 74–81. https://doi.org/10.1306/eg.11080505015

Holser, W.T. and Wilgus, C.K. 1981. Bromide profiles of the Röt salt, Triassic of northern Europe, as evidence of its marine origin. Neues Jahrbuch für Mineralogie Monatshefte, 6, 267–276.

Hossain, S., Hampson, G.J., Jacquemyn, C., Jackson, M.D. and Chiarella, D. 2024. Permeability characterisation of sedimentological facies in the Bunter Sandstone Formation, Endurance CO_2

ACCEPTED MANUSCRIPT

Downloaded from https://www.lyellcollection.org by UK Research and Innovation (UKRI/BGS/BAS) on Mar 09, 2026

storage site, offshore UK. International Journal of Greenhouse Gas Control, 135, 104140. https://doi.org/10.1016/j.ijggc.2024.104140

IEAGHG. 2011. Caprock Systems for CO_2 Geological Storage. International Energy Agency Greenhouse Gas R&D Programme, report, 2011-01. May 2011. Available at: https://ieaghg.org/publications/caprock-systems-for-co2-geological-storage/

ISO. 2017. Carbon dioxide capture, transportation and geological storage — Geological storage. International Organization for Standardization. ISO 27914:2017. Available at https://www.iso.org/standard/64148.html

Iglauer, S., Pentland, C.H. and Busch, A. 2015. CO_2 wettability of seal and reservoir rocks and the implications for carbon geo-sequestration. Water Resources Research, 51, 729–774. https://doi.org/10.1002/2014WR015553

Johnson, H., Warrington, G. and Stoker, S.J. 1994. Permian and Triassic of the Southern North Sea. In: Knox, R.W.O'B. and Cordey, W.G. (Eds.), Lithostratigraphic nomenclature of the UK North Sea. British Geological Survey on behalf of the UK Offshore Operators Association, 6.

Kovalevych, V., Peryt, T.M., Beer, W., Geluk, M. and Hałas, S. 2002. Geochemistry of Early Triassic seawater as indicated by study of the Röt halite in the Netherlands, Germany, and Poland. Chemical Geology, 182, 549–563. https://doi.org/10.1016/S0009-2541(01)00343-6

Kutzback, J.E. and Gallimore, R.G. 1989. Pangaean climates: Megamonsoons of the megacontinent. Journal of Geophysical Research, 94, 3341–3357. https://doi.org/10.1029/JD094iD03p03341

Loizzo, M., Houghton, R.D., Zahmul, A.H., Tonning, S.A. and Andersen, L.W. 2024. A Deeper Understanding of the Role of Salts and Creeping Formations in Well Integrity. In: SPE-220070-MS, Presented at the SPE Europe Energy Conference and Exhibition, Turin, Italy, 26–28 June 2024. https://doi.org/10.2118/220070-MS

Martin-Clave, C., Ougier-Simonin, A. and Vandeginste, V. 2021. Impact of Second Phase Content on Rock Salt Rheological Behavior Under Cyclic Mechanical Conditions. Rock Mechanics and Rock Engineering, 54, 5245–5267. https://doi.org/10.1007/s00603-021-02449-4

Milroy, P., Wright, P. and Simms, M.J. 2019. Dryland continental mudstones: Deciphering environmental changes in problematic mudstones from the Upper Triassic (Carnian to Norian) Mercia Mudstone Group, south-west Britain. Sedimentology, 66, 2557–2589. https://doi.org/10.1111/sed.12626

ACCEPTED MANUSCRIPT

Downloaded from https://www.lyellcollection.org by UK Research and Innovation (UKRI/BGS/BAS) on Mar 09, 2026

National Grid. 2016. K40: Subsurface Geoscience and Production Chemistry Reports. Technical: Storage. February 2016. Available at https://assets.publishing.service.gov.uk/media/5a7f8d2440f0b62305b87d51/K40_Subsurface_Geoscience_and_Production_Chemistry.pdf

Newell, A.J. 2018. Rifts, rivers and climate recovery: A new model for the Triassic of England. Proceedings of the Geologist's Association, 129 (3), 352–371. https://doi.org/10.1016/j.pgeola.2017.04.001

Noy, D.J., Holloway, S., Chadwick, R.A., Williams, J.D.O., Hannis, S.A. and Lahann, R.W. 2012. Modelling large-scale carbon dioxide injection into the Bunter Sandstone in the UK Southern North Sea. International Journal of Greenhouse Gas Control, 9, 220–233. https://doi.org/10.1016/j.ijggc.2012.03.011

Parrish, J.T. 1993. Climate of the Supercontinent Pangea. The Journal of Geology, 101, 215–233. https://doi.org/10.1086/648217

Patruno, S., Green, A., Corcoran, J., Caldarella, D., Scisciani, V. and Przywara, M. 2024. A conceptual CO_2 fill-and-spill mega-fairway in the UK Southern North Sea: A new approach to identify and optimise large-scale underground carbon storage (CCS). International Journal of Greenhouse Gas Control, 133, 104092. https://doi.org/10.1016/j.ijggc.2024.104092

Peach, C.J. and Spiers, C. 1996. Influence of crystal plastic deformation on dilatancy and permeability development in synthetic salt rock. Tectonophysics, 256, 101–128. https://doi.org/10.1016/0040-1951(95)00170-0

Popp, T., Kern, H. and Schulze 2001. Evolution of dilatancy and permeability in rock salt during hydrostatic compaction and triaxial deformation. Journal of Geophysical Research, 106, B3, 4061–4078. https://doi.org/10.1029/2000JB900381

Riddler, G.P. 1981. The distribution of the Röt Halite Member in North Yorkshire, Cleveland and North Humberside. Proceedings of the Yorkshire Geological Society, 43, 341–346. https://doi.org/10.1144/pygs.43.3.341

Ruffell, A. and Hounslow, M. 2006. Triassic: seasonal rivers, dusty deserts and saline lakes. In: Rawson, P.F. and Brenchley, P. (Eds.), The Geology of England and Wales. Geological Society, London, 295–325.

ACCEPTED MANUSCRIPT

Downloaded from https://www.lyellcollection.org by UK Research and Innovation (UKRI/BGS/BAS) on Mar 09, 2026

Ruffell. A. and Kürschner, W. M. 2020. Sediment Cyclicity and the Carnian Pluvial Episode: Evidence from Spectral Gamma-ray Logging of the Mercia Mudstone Group, SW England. Boletín Geológico y Minero, 131 (2), 231–242. https://doi.org/10.21701/bolgeomin.131.2.002

Rushton, J.C., Hannis, S., Pearce, J., Williams, J. and Milodowski, A.E. 2025. Diagenetic evolution of the Bunter Sandstone Formation and its controls on reservoir quality: Implications for CO_2 injectivity and storage. Geoenergy, 3, 2024-023. https://doi.org/10.1144/geoenergy2024-023

Salisbury, J., Gröcke, D.R. and McKie, T. 2023. Sulphur isotope stratigraphy of drill cuttings and stratigraphic correlation of Permian-Triassic evaporites. Frontiers in Earth Science, 11, 1216365. https://doi.org/10.3389/feart.2023.1216365

Schulze, O., Popp, T. and Kern, H. 2001. Development of damage and permeability in deforming rock salt. Engineering Geology, 61 (2–3), 163–180. https://doi.org/10.1016/S0013-7952(01)00051-5

Seedhouse, J.K. and Racey, A. 1997. Sealing capacity of the Mercia Mudstone Group in the East Irish Sea Basin: Implications for petroleum exploration. Journal of Petroleum Geology, 20, 261–286. https://doi.org/10.1111/j.1747-5457.1997.tb00636.x

Shoulders, S. and Hodgkinson, J. 2024. A process-led approach to framing uncertainty and risk in CO_2 storage in the subsurface. Geoenergy, 2, 2024-11. https://doi.org/10.1144/geoenergy2024-011

Southworth, C.J. 1987. Lithostratigraphy and depositional history of the Middle Triassic Dowsing Dolomitic Formation of the Southern North Sea and adjoining areas. PhD thesis, University of Oxford. Available at Oxford University Research Archive: https://ora.ox.ac.uk/objects/uuid:5a6eee8b-9ab9-4b94-91f9-2ed4b36da98f

Spain, J.D. and Conrad, C.P. 1997. Quantitative analysis of top-seal capacity: Offshore Netherlands, Southern North Sea. Geologie en Mijnbouw, 76, 217–226. https://doi.org/10.1023/A:1003056609771

Span, R. and Wagner, W. 1996. A new equation of state for carbon dioxide covering the fluid region from the triple-point temperature to 1100 K at pressures up to 800 MPa. Journal of Physical and Chemical Reference Data, 25, 1509–1596. https://doi.org/10.1063/1.555991

Stewart, S.A. and Coward, M.P. 1995. Synthesis of salt tectonics in the southern North Sea, UK. Marine and Petroleum Geology, 12, 457–475. https://doi.org/10.1016/0264-8172(95)91502-G.

Underhill, J.R. 2003. The tectonic and stratigraphic framework of the United Kingdom's oil and gas fields. In: Gluyas, J.G. and Hichens, H.M. (Eds.), United Kingdom Oil and Gas Fields, Commemorative

ACCEPTED MANUSCRIPT

Downloaded from https://www.lyellcollection.org by UK Research and Innovation (UKRI/BGS/BAS) on Mar 09, 2026

Millennium Volume. Geological Society, London, Memoirs, 20, 17–59. https://doi.org/10.1144/GSL.MEM.2003.020.01.04

Underhill, J.R. 2009. Role of intrusion-induced salt mobility in controlling the formation of the enigmatic 'Silverpit Crater', UK Southern North Sea. Petroleum Geoscience, 15, 197–216. https://doi.org/10.1144/1354-079309-843

Underhill, J.R., de Jonge-Andersen, I., Hollinsworth, A.D. and Fyfe, L.C. 2023. Use of exploration methods to repurpose and extend the life of a super basin as a carbon storage hub for the energy transition. AAPG Bulletin, 107 (8), 1419–1474. https://doi.org/10.1306/04042322097

Van Hoorn, B. 1987. Structural evolution, timing and tectonic style of the Sole Pit inversion. Tectonophysics, 137, 239–284. https://doi.org/10.1016/0040-1951(87)90322-2.

Warren, J.K. 2016. Evaporites: A Compendium. Springer, Berlin. 1854 pp.

Warren, J.K. 2017. Salt usually seals, but sometimes leaks: Implications for mine and cavern stabilities in the short and long term. Earth-Science Reviews, 165, 302–341. https://doi.org/10.1016/j.earscirev.2016.11.008

Williams, J.D.O., Bentham, M., Jin, M., Pickup, G., Mackay, E., Gammer, D. and Green, A. 2013a. The effect of geological structure and heterogeneity on CO_2 storage in simple 4-way dip structures; a modelling study from the UK Southern North Sea. Energy Procedia, 37, 3980–3988. https://doi.org/10.1016/j.egypro.2013.06.297

Williams, J.D.O., Holloway, S. and Williams, G.A. 2014. Pressure constraints on the CO_2 storage capacity of the saline water-bearing parts of the Bunter Sandstone Formation in the UK Southern North Sea. Petroleum Geoscience, 20, 155–167. https://doi.org/10.1144/petgeo2013-019

Williams, J.D.O., Jin, M., Bentham, M., Pickup, G.E., Hannis, S.D. and Mackay, E.J. 2013b. Modelling carbon dioxide storage within closed structures in the UK Bunter Sandstone Formation. International Journal of Greenhouse Gas Control, 18, 38–50. https://doi.org/10.1016/j.ijggc.2013.06.015

Williams, J.D.O., Williams, G.A., Fellgett, M.W., Abel, L. and Bridger, P. Submitted, this volume. Regional geomechanical response to large-scale CO_2 storage in the Bunter Sandstone, UK Southern North Sea. Geoenergy.

Zhang, Q., Liu, J., Wang, L., Luo, M., Liu, H., Xu, H. and Zou, H. 2020. Impurity Effects on the Mechanical Properties and Permeability Characteristics of Salt Rock. Energies, 13 (6), 1366. https://doi.org/10.3390/en13061366

ACCEPTED MANUSCRIPT

Downloaded from https://www.lyellcollection.org by UK Research and Innovation (UKRI/BGS/BAS) on Mar 09, 2026

Ziegler, W. 1975. Outline of the Geological History of the North Sea. In: Woodland, A.W. (Ed.), Petroleum and the Continental Shelf of Northwest Europe; the geology and the environment Vol. 1. Geology. Applied Science Publishers, 165-187

Ziegler, P.A. 1990. Geological Atlas of Western and Central Europe. Second edition. Shell Internationale Petroleum Maatschappij B.V., The Hague.

ACCEPTED MANUSCRIPT

Downloaded from https://www.lyellcollection.org by UK Research and Innovation (UKRI/BGS/BAS) on Mar 09, 2026

Table 1. Summary of number of wells where the RHM is present, and also where the RHM is absent due either to lack of deposition or post-depositional erosion, faulting or invasion by Zechstein salts.

	RHM present	Faulted out	Invaded by Zechstein salts	Absent (lack of deposition or post-depositional erosion)
Number of wells	398	11	28	163

ACCEPTED MANUSCRIPT

Downloaded from https://www.lyellcollection.org by UK Research and Innovation (UKRI/BGS/BAS) on Mar 09, 2026

Fig. 1. Location map showing the extent of the Bunter Sandstone in the UKSNS (after Cameron et al., 1992), major structural elements, including Zechstein salt wall structures that penetrate the Bunter Sandstone (after Abel et al., 2025), and carbon storage licence areas. Offshore quadrant, CO_2 storage licence and coastline linework contains information provided by the North Sea Transition Authority and/or other third parties (https://opendata-nstauthority.hub.arcgis.com/search).

Fig. 2. (a) Tectonostratigraphic chart for the UK Southern North Sea, adapted from Abel et al. (2025). The tectonic history was compiled from Glennie (1990), Doornenbal and Stevenson (2010) and Grant et al. (2019; 2020). MMU: Mid Miocene Unconformity, BCU: Base Cretaceous Unconformity, BPU: Base Permian Unconformity. (b) Stratigraphic detail for the Haisborough Group indicating position of the Röt Halite Member within the Dowsing Formation (after Johnson et al., 1994).

Fig. 3. Comparison of stratigraphic schemes for the UK Dowsing Formation, after Johnson et al. (1994) and Southworth (1987), and the Netherlands scheme as summarised by Geluk and Röhling (1997).

Fig. 4. Typical petrophysical log response from the RHM and surrounding strata. The example is taken from the 42/25d-3 Endurance appraisal well (Figure 1). FIT: Formation Integrity Test. EMW: Equivalent Mud Weight in pounds per gallon (ppg). The nomenclature used to characterise the units overlying the RHM follows Southworth (1987). Contains information provided by the North Sea Transition Authority and/or other third parties (https://ndr.nstauthority.co.uk/).

Fig. 5. Cross sections A-A' (SW-NE), B-B' (W-E), and C-C' (SE-NW), flattened to the top Main REM. Locations of cross sections are shown on Figure 6. Contains information provided by the North Sea Transition Authority and/or other third parties (https://ndr.nstauthority.co.uk/).

Fig. 6. RHM distribution map for the UKSNS and adjacent regions, including distribution of wells in which the RHM is present and/or absent. Wells within the RHM depositional extent, where the RHM is absent due to faulting, intrusion by mobile Zechstein salts, and erosion are also shown. Location of Figure 5 cross-sections are also shown. Offshore quadrant, wells and coastline linework contains information provided by the North Sea Transition Authority and/or other third parties (https://opendata-nstauthority.hub.arcgis.com/search).

Fig. 7. Distribution and thickness of individual evaporite cycles A–E interpreted from well log data within the RHM of the UKSNS. Relevant regional structural features are shown in Figure 1. Offshore quadrant, wells and coastline linework contains information provided by the North Sea Transition Authority and/or other third parties (https://opendata-nstauthority.hub.arcgis.com/search).

ACCEPTED MANUSCRIPT

Downloaded from https://www.lyellcollection.org by UK Research and Innovation (UKRI/BGS/BAS) on Mar 09, 2026

Fig. 8. Optical photomicrograph in partially crossed polarised light showing outline of relict primary chevron halite (H) crystal defined by fluid inclusions (F). These inclusions are now enclosed in a coarse halite with different crystallographic boundaries indicating recrystallisation. A patch of primary mudstone is rimmed by bright anhydrite (A). BGS thin section SSK151437, sampled from Cycle B in the well 42/25d-3.

Fig. 9. Cumulative depositional thickness map of the Main RHM. Wells within the RHM depositional extent, but where the RHM is absent due to faulting, intrusion by mobile Zechstein salts, and erosion are also differentiated. These wells were excluded from the gridding process. Offshore quadrant, wells, and coastline linework contain information provided by the North Sea Transition Authority and/or other third parties (https://opendata-nstauthority.hub.arcgis.com/search).

Fig. 10. Map illustrating the number of Main RHM cycles across the UKSNS, overlain by current carbon storage licence boundaries (labels refer to North Sea Transition Authority licence numbers). Offshore quadrant, carbon storage licence and coastline linework contains information provided by the North Sea Transition Authority and/or other third parties (https://opendata-nstauthority.hub.arcgis.com/search).

Fig. 11. Variation in deformation styles observed in the overburden to the BSF and the influence of the Röt Halite Member (modified from Abel et al., 2025). (a) throughgoing faults on the crest of a structural closure, (b) slumping on the flanks of a structural closure, (c) Zechstein salt intrusion utilising the plane of weakness of the RHM. Note: the RHM is located between the “Triassic: Bacton Group” and the “Triassic”. Location of seismic line shown on Figure 1. Seismic data contains information provided by the North Sea Transition Authority and/or other third parties (https://ndr.nstauthority.co.uk/).

Fig. 12. Maps illustrating closures in the underlying Bunter Sandstone Formation, taken from the CO_2Stored database. Closures are coloured to illustrate the relative degree of fault throw (left) or fault density (right), as categorised in the database. Offshore quadrant and coastline linework contains information provided by the North Sea Transition Authority and/or other third parties (https://opendata-nstauthority.hub.arcgis.com/search).

ACCEPTED MANUSCRIPT

Downloaded from https://www.lyellcollection.org by UK Research and Innovation (UKRI/BGS/BAS) on Mar 09, 2026

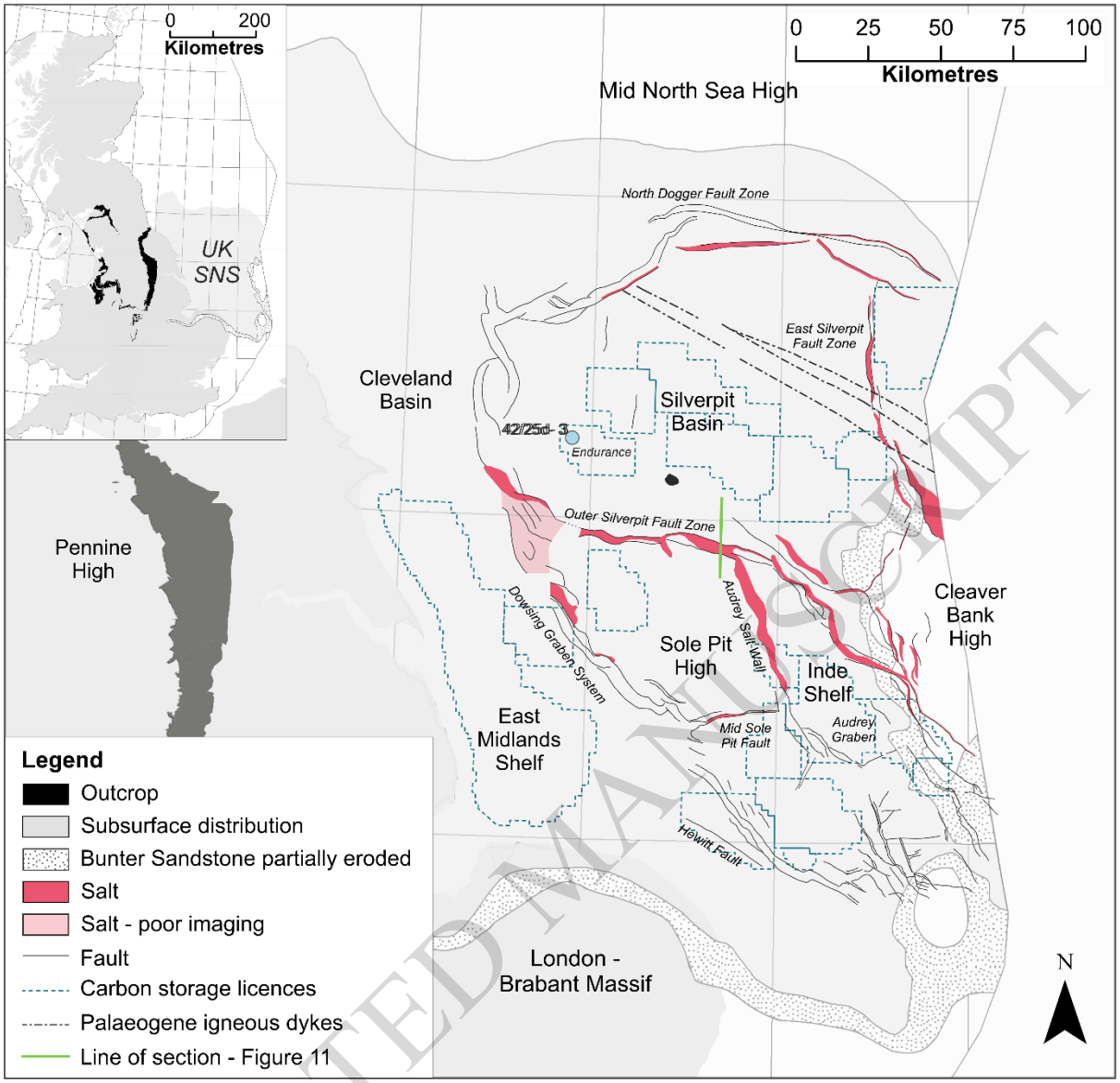

Figure 1

ACCEPTED MANUSCRIPT

Downloaded from https://www.lyellcollection.org by UK Research and Innovation (UKRI/BGS/BAS) on Mar 09, 2026

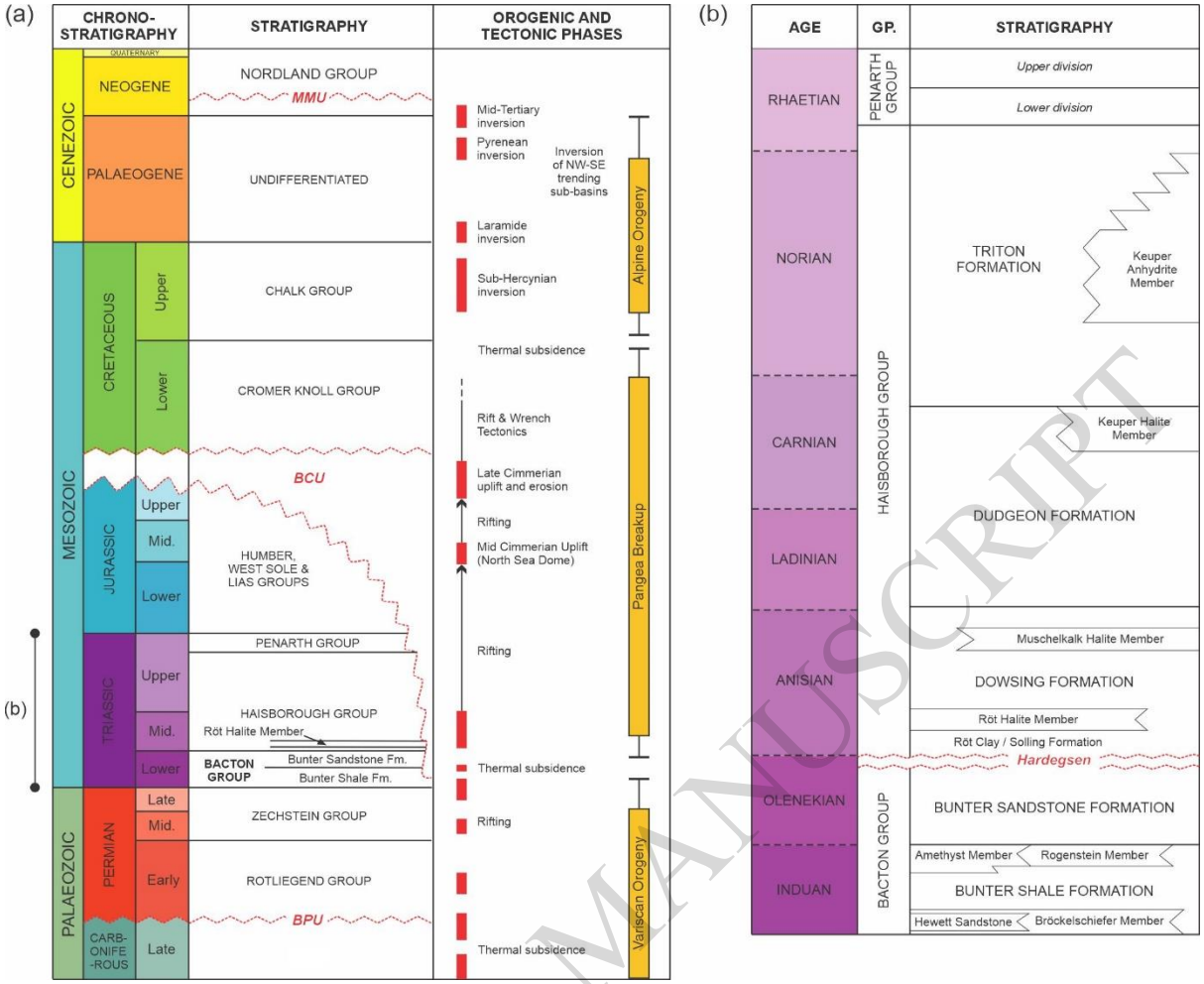

Figure 2

ACCEPTED MANUSCRIPT

Downloaded from https://www.lyellcollection.org by UK Research and Innovation (UKRI/BGS/BAS) on Mar 09, 2026

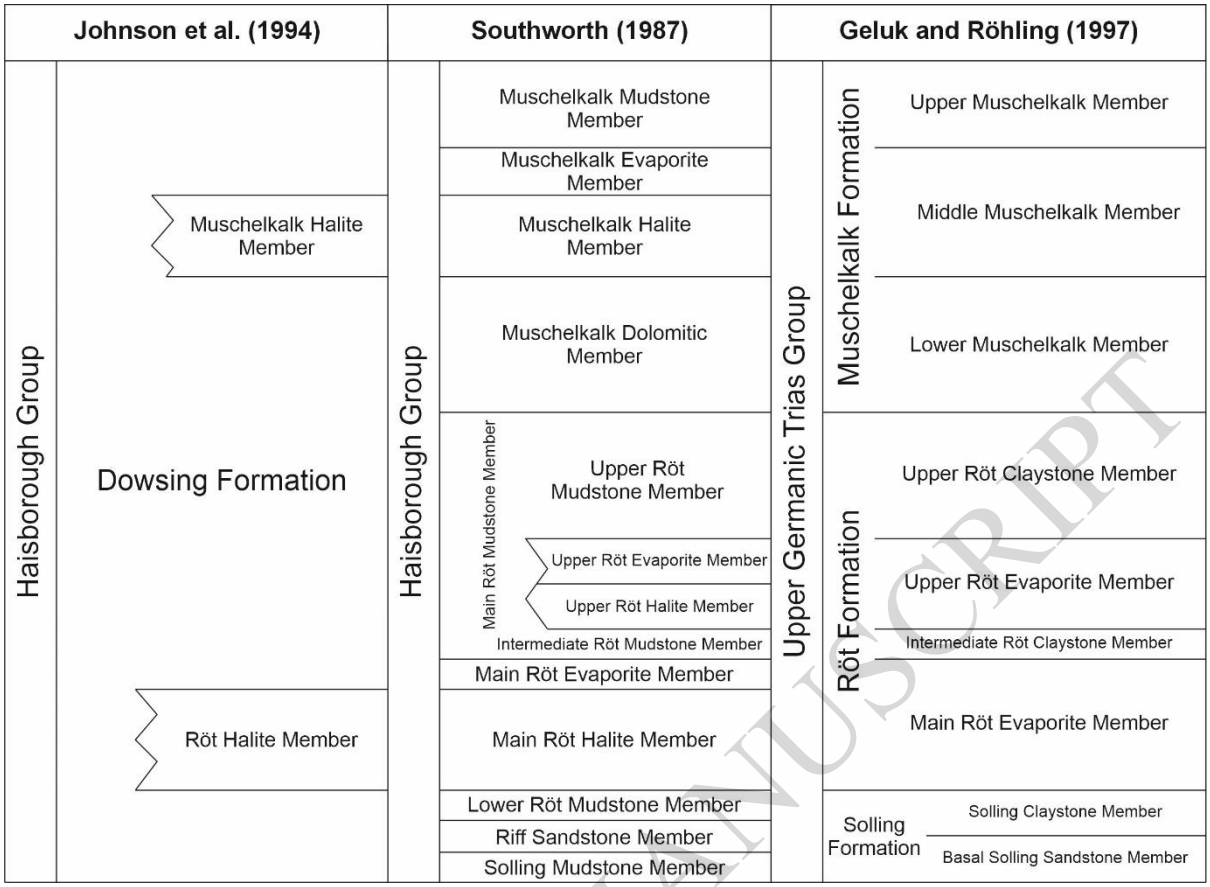

Figure 3

ACCEPTED MANUSCRIPT

Downloaded from https://www.lyellcollection.org by UK Research and Innovation (UKRI/BGS/BAS) on Mar 09, 2026

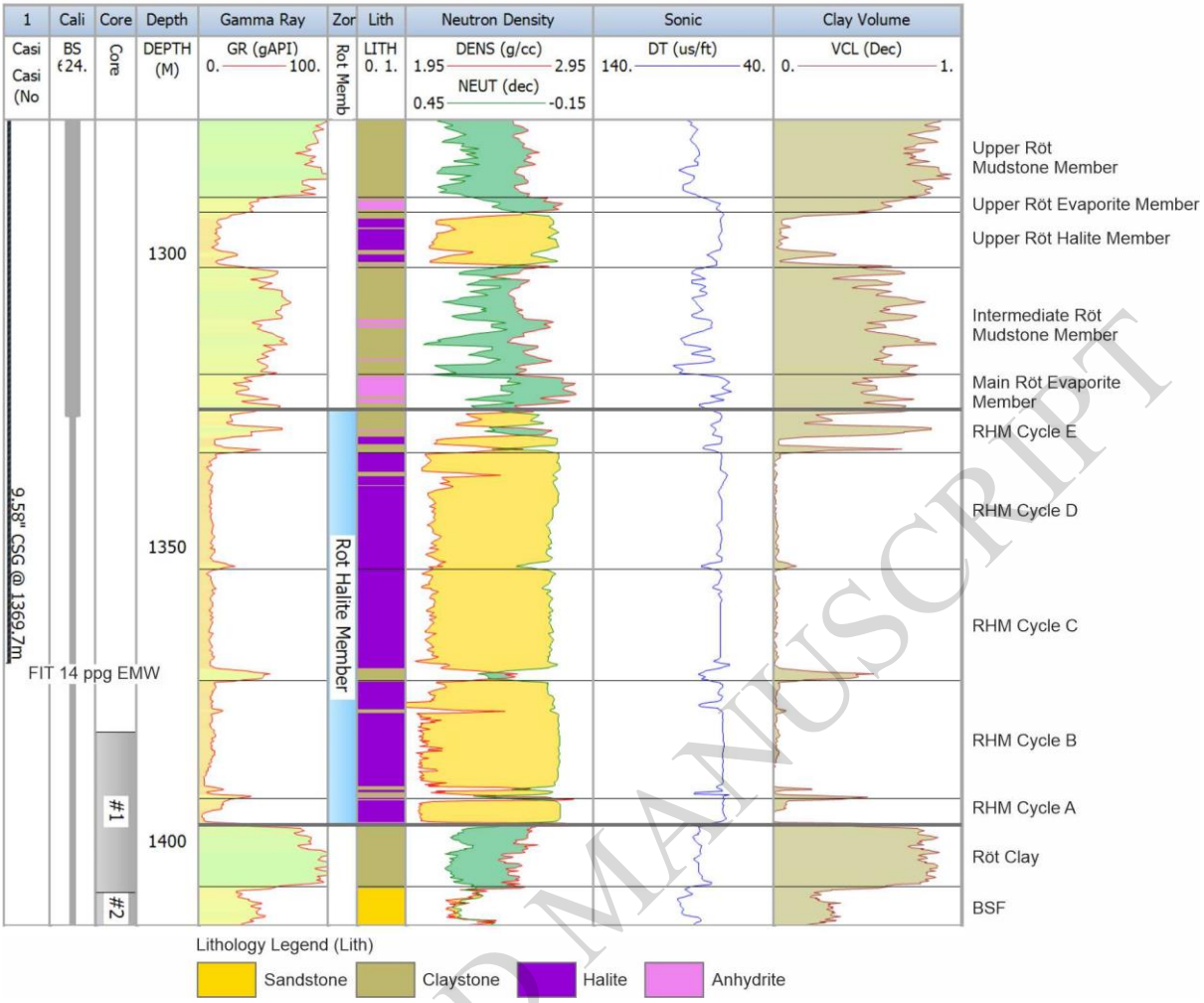

Figure 4

ACCEPTED MANUSCRIPT

Downloaded from https://www.lyellcollection.org by UK Research and Innovation (UKRI/BGS/BAS) on Mar 09, 2026

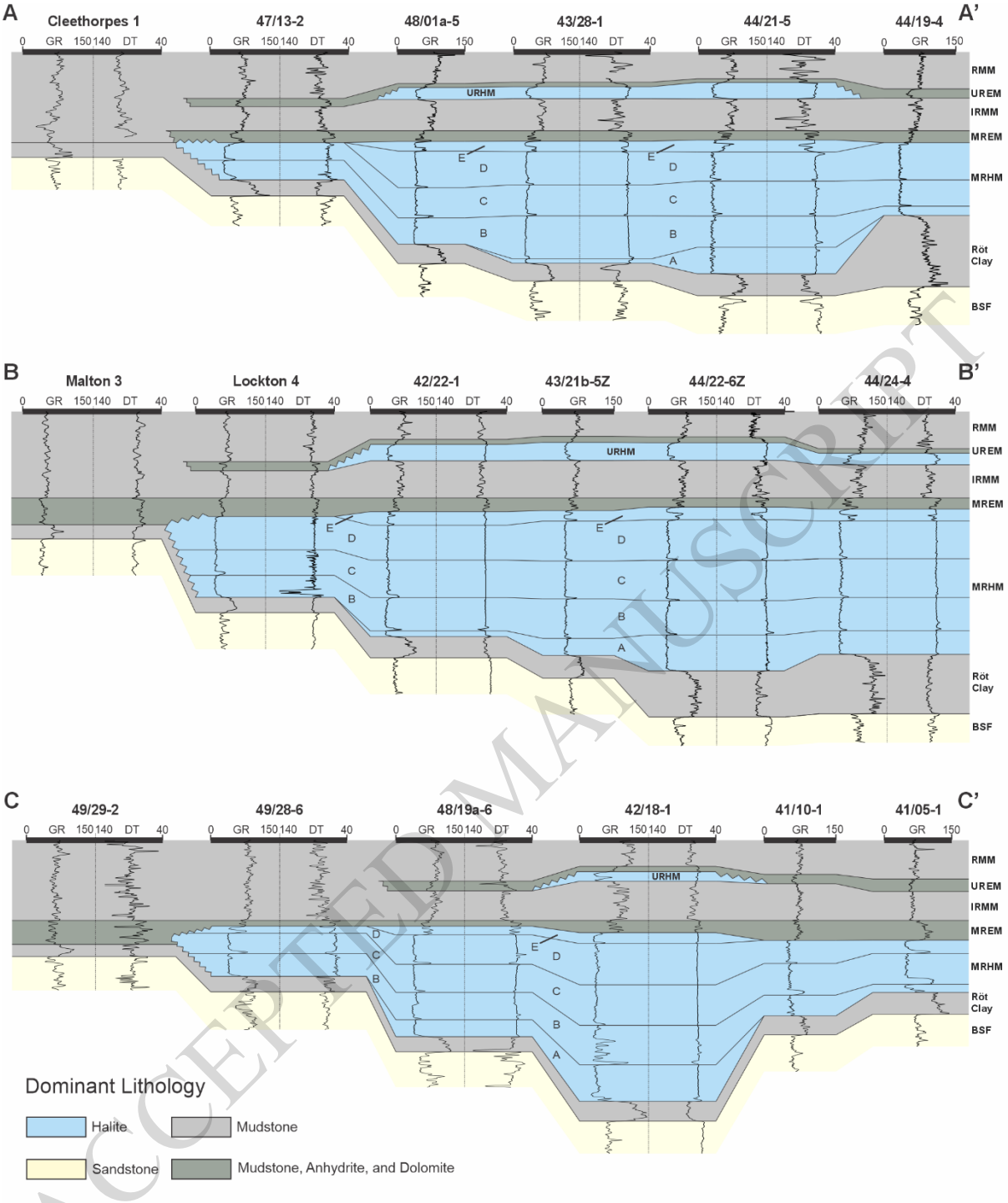

ACCEPTED MANUSCRIPT

Figure 5

Downloaded from https://www.lyellcollection.org by UK Research and Innovation (UKRI/BGS/BAS) on Mar 09, 2026

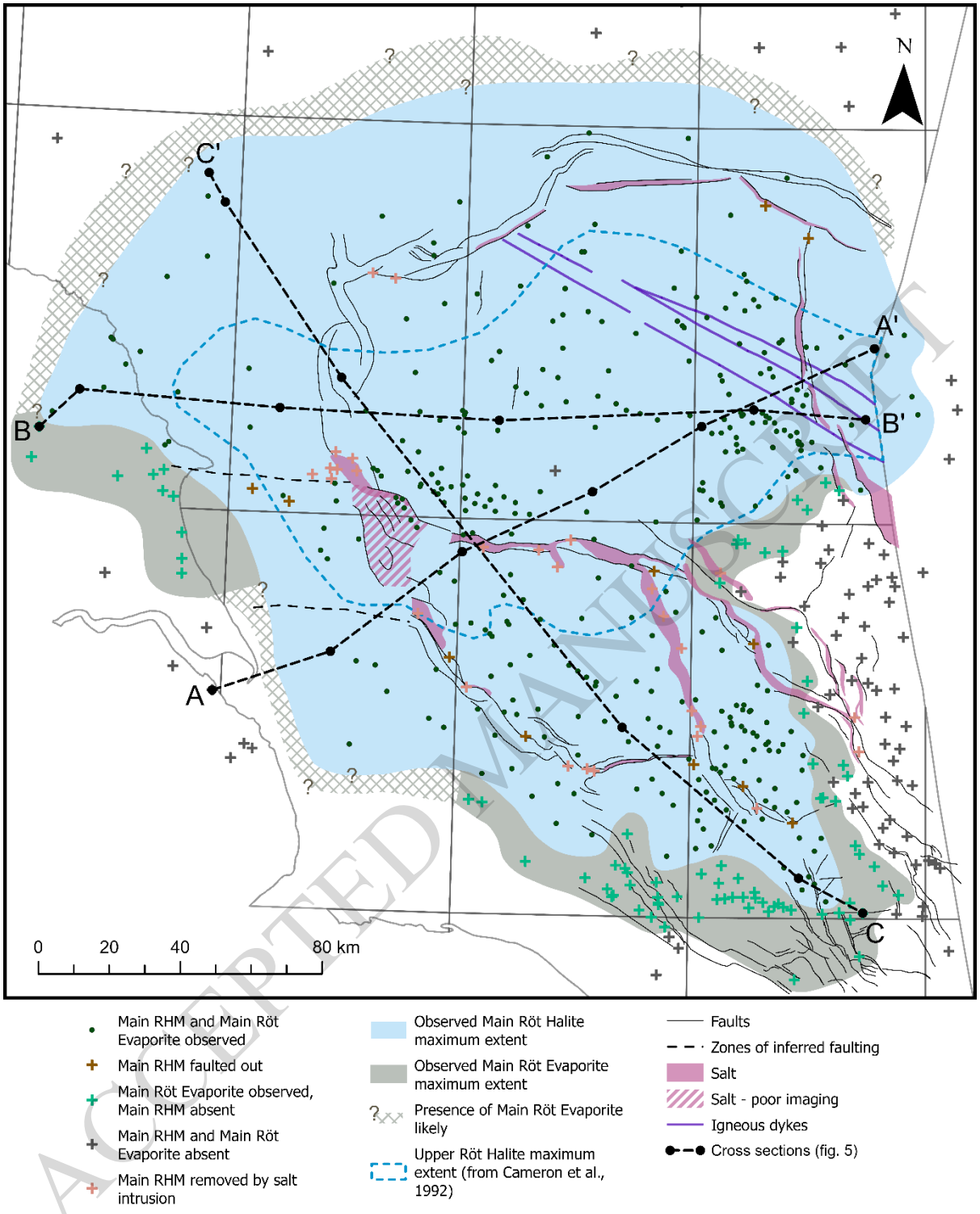

ACCEPTED MANUSCRIPT

Figure 6

Downloaded from https://www.lyellcollection.org by UK Research and Innovation (UKRI/BGS/BAS) on Mar 09, 2026

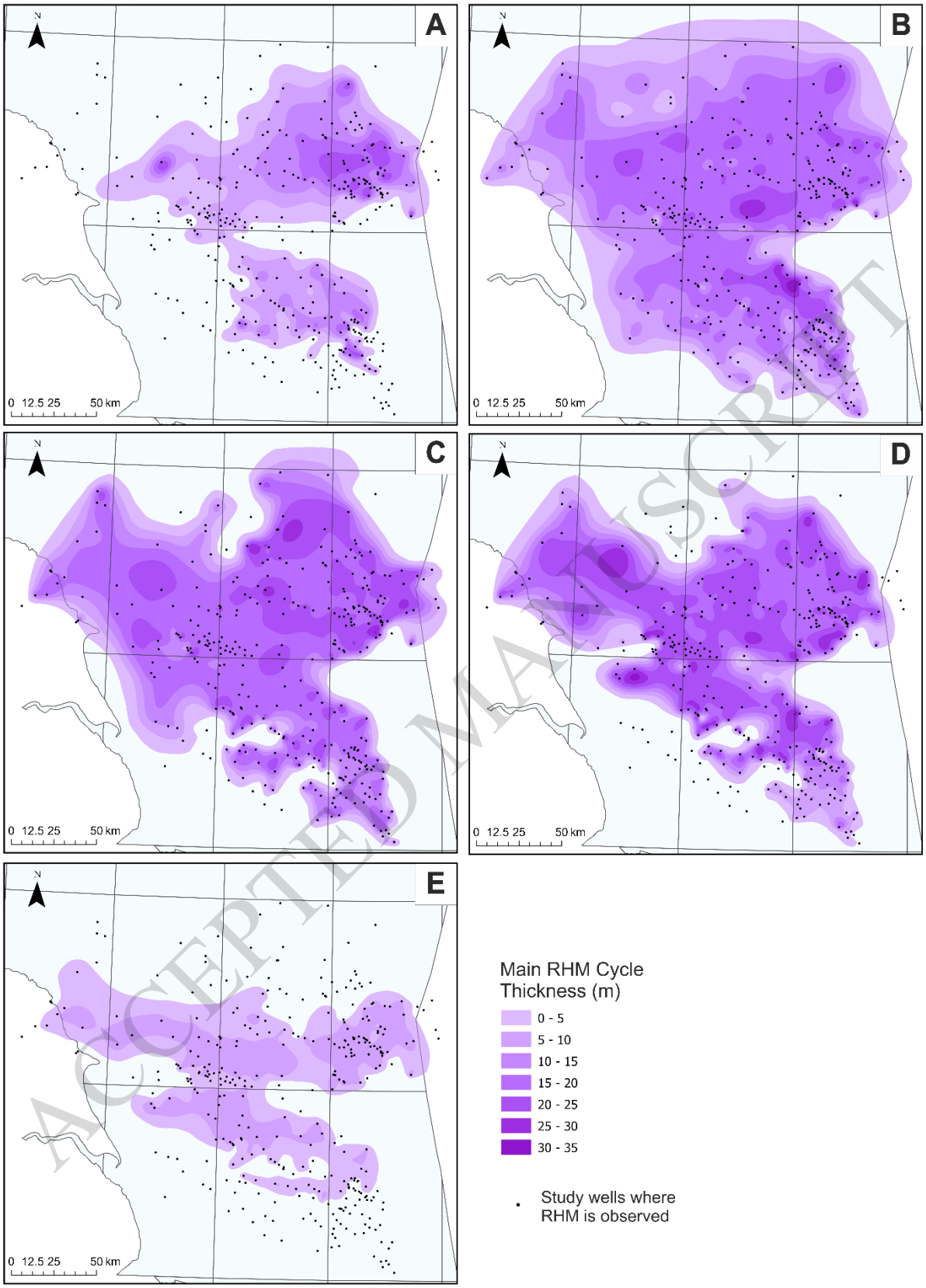

ACCEPTED MANUSCRIPT

Figure 7

Downloaded from https://www.lyellcollection.org by UK Research and Innovation (UKRI/BGS/BAS) on Mar 09, 2026

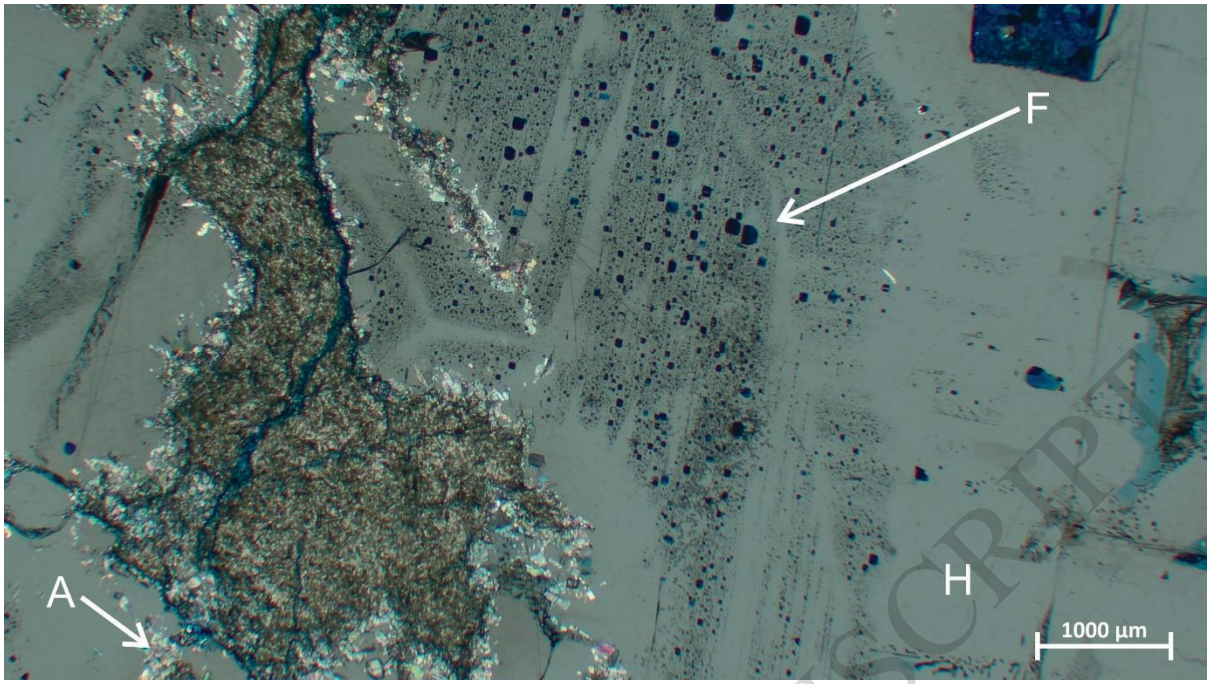

Figure 8

ACCEPTED MANUSCRIPT

Downloaded from https://www.lyellcollection.org by UK Research and Innovation (UKRI/BGS/BAS) on Mar 09, 2026

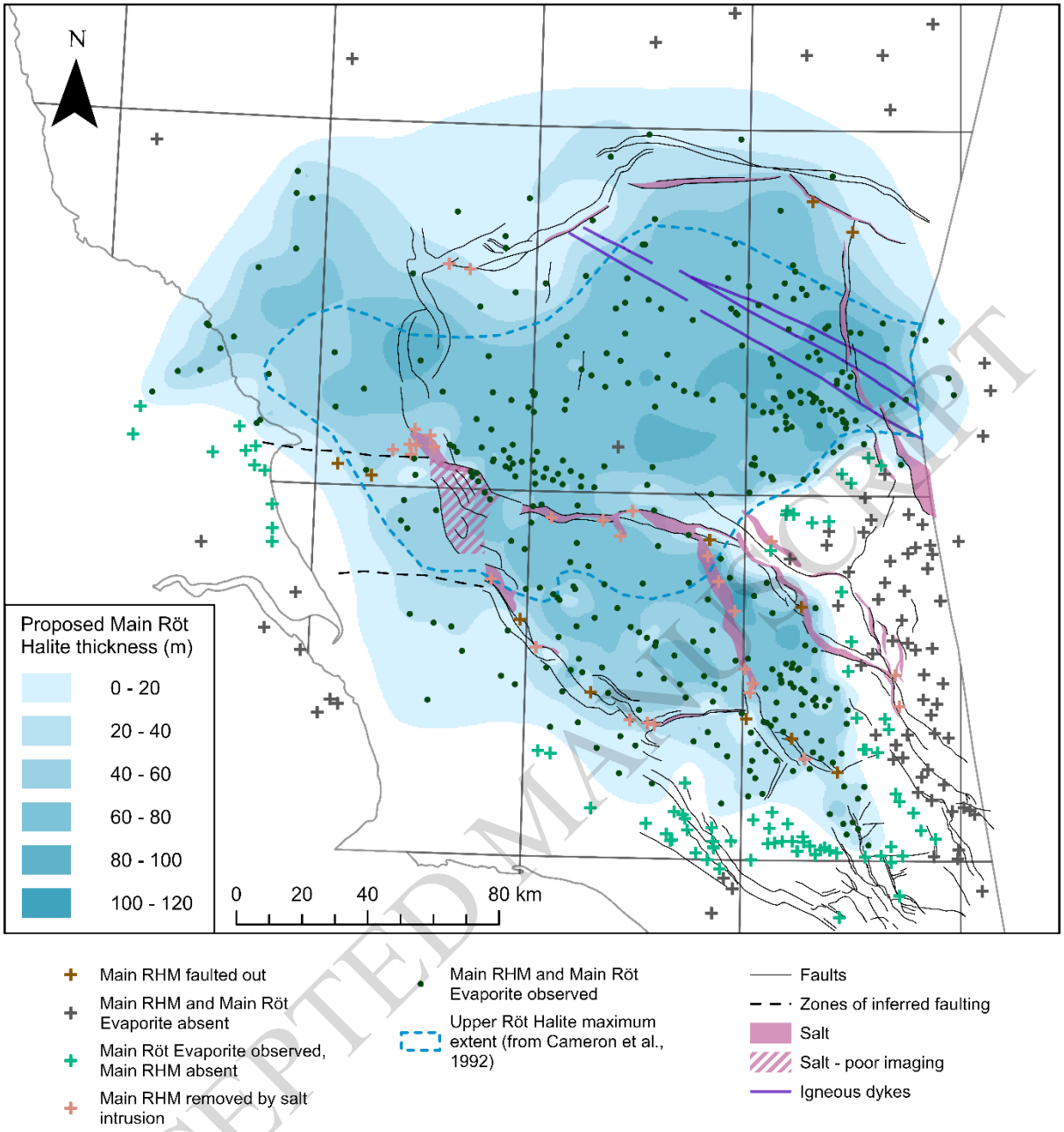

Figure 9

ACCEPTED MANUSCRIPT

Downloaded from https://www.lyellcollection.org by UK Research and Innovation (UKRI/BGS/BAS) on Mar 09, 2026

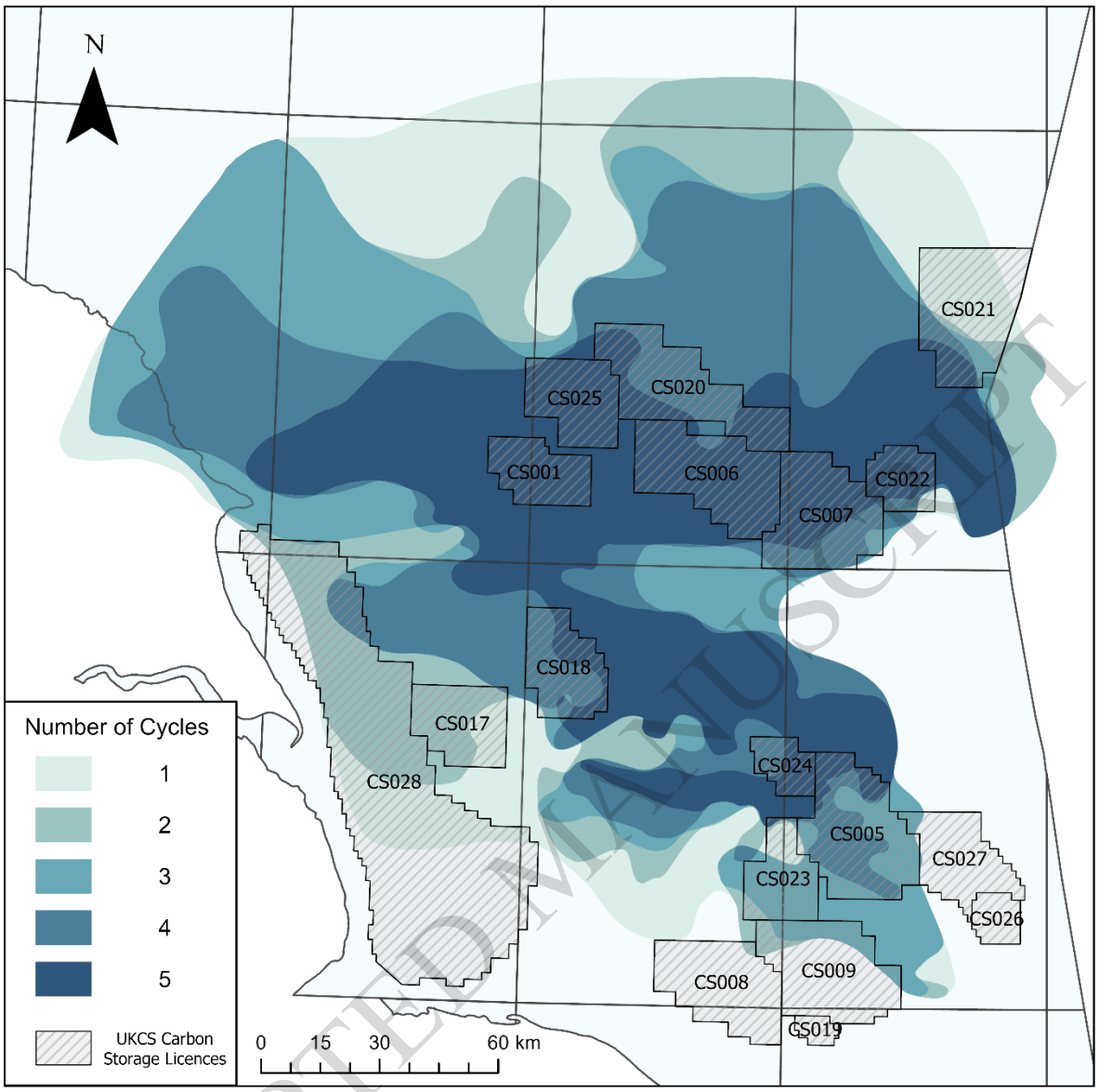

Figure 10

ACCEPTED MANUSCRIPT

Downloaded from https://www.lyellcollection.org by UK Research and Innovation (UKRI/BGS/BAS) on Mar 09, 2026

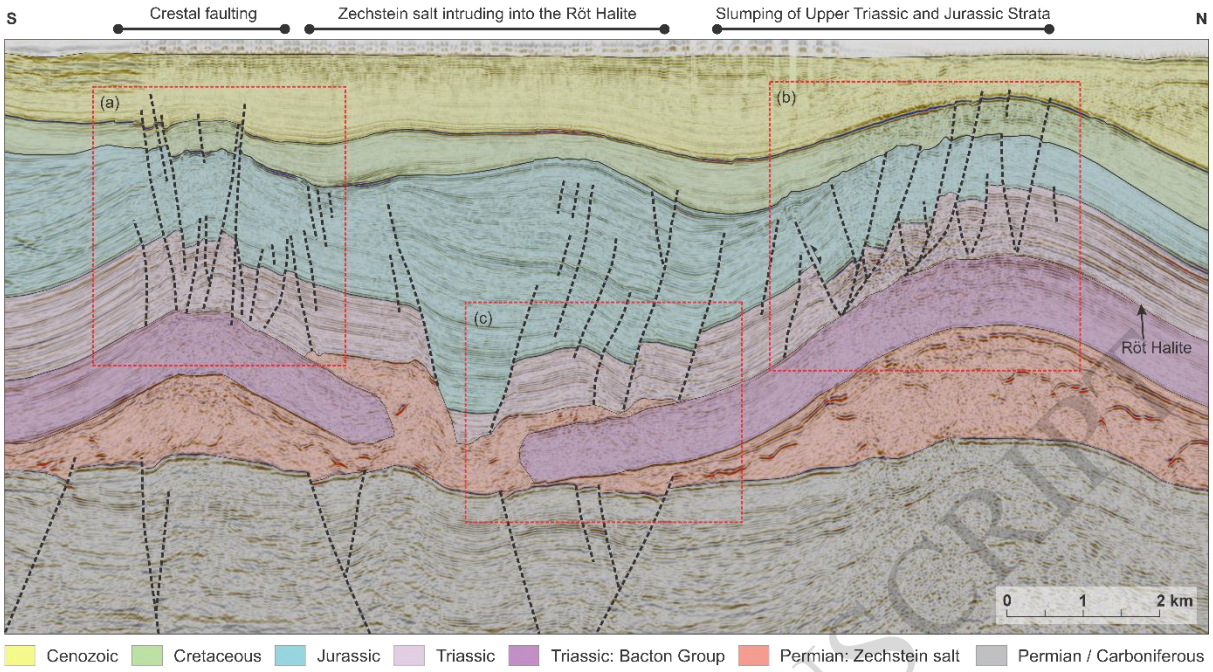

Figure 11

ACCEPTED MANUSCRIPT

Downloaded from https://www.lyellcollection.org by UK Research and Innovation (UKRI/BGS/BAS) on Mar 09, 2026

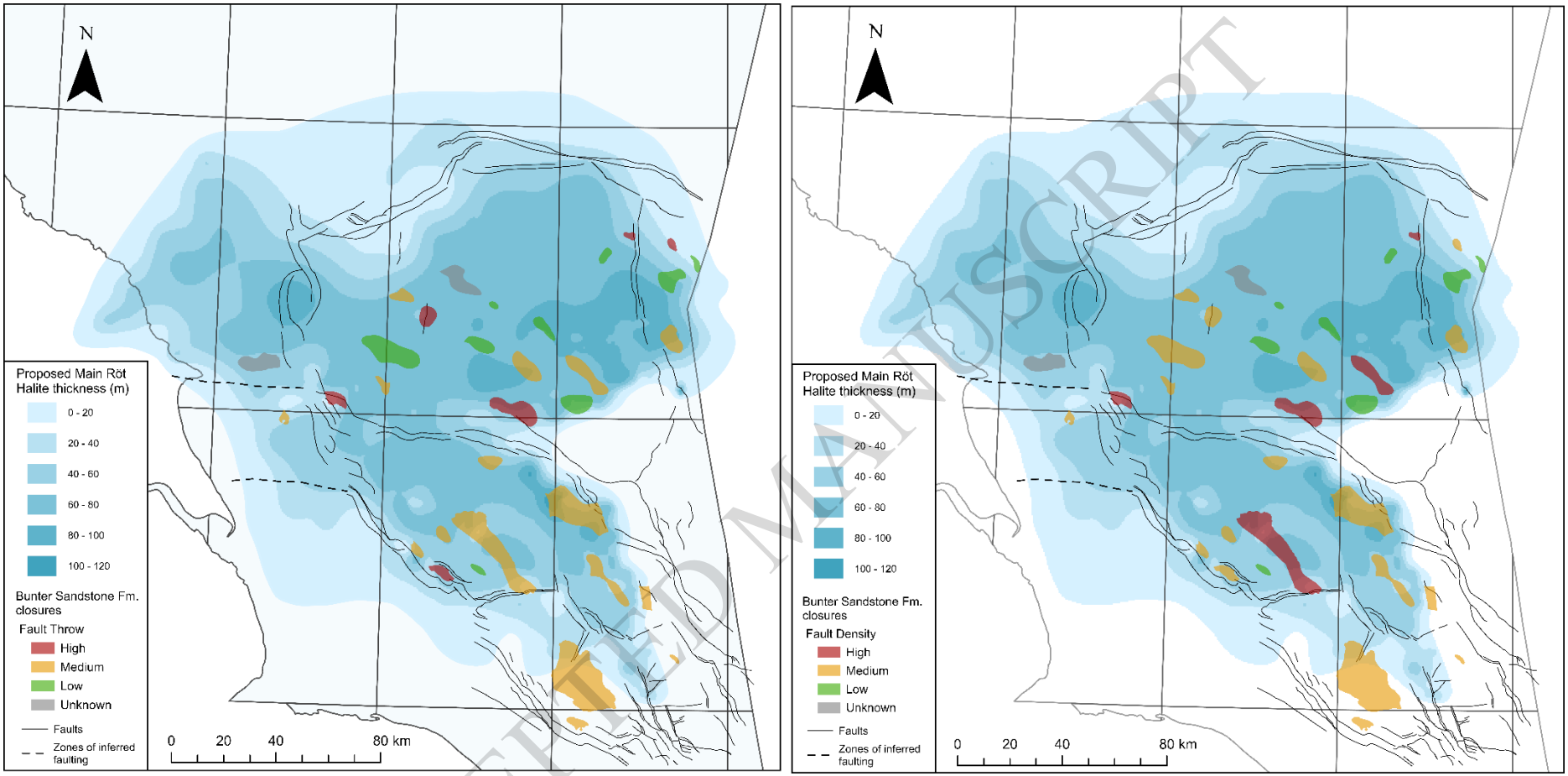

Figure 12

ACCEPTED MANUSCRIPT